



? g ^f[V[eU[b ^ Sdk EfdgUfgdS^3` S^ke[e
S` V 6d[^ Y FSdYWfe Sf · W[efSdWk] [d

@adfZWd D[X La` WS` V Föd W 8dSufgdWLa` W

LV-2015-135



Multidisciplinary Structural Analysis and Drilling Targets at Þeistareykir

Northern Rift Zone and Tjörnes Fracture Zone



ÍSOR-2015/043

Project no.: 15-0104

December 2015

Key Page



LV report no: LV-2015-135 **Date:** December 2015

Number of pages: 49 +
1 map **Copies:** 11 **Distribution:** On www.lv.is
 Open
 Limited until

Title: Multidisciplinary structural analysis and drilling targets at Þeistareykir

Authors/Company: Maryam Khodayar, Sveinbjörn Björnsson, Sigurður G. Kristinsson,
Ragna Karlsdóttir and Magnús Ólafsson

Project manager: Ásgrímur Guðmundsson (LV) Magnús Ólafsson (ÍSOR)

Prepared for: Prepared by Iceland GeoSurvey (ÍSOR) for Landsvirkjun.

Co operators: _____

Abstract: Results of Phase 3 of the multidisciplinary structural analysis of Þeistareykir and surroundings are presented here. A number of data such as previous drilling targets, potential permeable fractures as paths for feeders in wells, formation temperatures, and resistivity are analysed and correlated with the structural map made in Phase 1. The goal is to provide new insights into the combined tectonic of rift and transform zones in North Iceland, which controls the geological processes and geothermal activity. Results are used to suggest the best potential targets for drilling. The main results of this analysis and correlations are: (a) A higher number of fractures, belonging to both the rift and transform plate boundaries, seems to be present at depth in the areas of the 10 previous drilled exploration/production wells. (b) The analysis of feeders and the fracture pattern shows that the Riedel shears of the transform zone such as the dextral WNW and NW, as well as the sinistral ENE oblique-slip faults are the main permeable fractures, in addition to a few shorter northerly segments. These are the same sets, and in some cases the same fractures that bound the alteration block, let gases seep through the surface, compartmentalise the formation temperatures in the geothermal reservoir, and control the resistivity anomalies. (c) Among the Riedel shears, few play more critical roles. As examples, the WNW Stórhver-Bæjarfjall dextral fault shifts the entire Þeistareykir fissure swarm. Its splay segment enters the reservoir so that the northerly segments to its north are not the continuation of the northerly segments to its south. A few of the ENE weak zones cutting the northern part of the Bæjarfjall and its northern slope are among the most critical structures for geothermal activity. (d) Based on the identified fracture sets of the rift and transform zones, five areas are suggested for drilling. The central area coincides with the up-flow zone from the reservoir and should provide the best production. The other four surrounding areas are the best candidates for exploration drillings. Several of the northerly rift-parallel and Riedel shears of transform zones are selected as structural targets within each of the five areas. These structures are mostly fracture intersections but also a few fracture traces.

Keywords: Northern Rift Zone; Tjörnes Fracture Zone; Fracture permeability; Formation temperatures; resistivity; Drilling; Tectonic

ISBN no: _____

Approved by Landsvirkjun's project manager

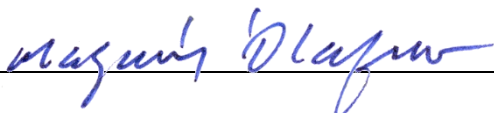
Project manager's signature 	Reviewed by Sigvaldi Thordarson
--	------------------------------------

Table of Contents

1	Introduction	7
2	Geological settings.....	8
2.1	The general context.....	8
2.2	Recall of the structural re-evaluation of Þeistareykir.....	9
3	Previous drilling targets at Þeistareykir	10
4	New structural analysis of borehole data.....	11
4.1	Feeders and fractures in existing wells	11
4.2	Formation temperature	12
4.3	Structural provinces of formation temperatures	13
5	Multidisciplinary data correlation and modelling.....	14
5.1	Correlation of borehole data with results of Phases 1 and 2.....	14
5.2	Further correlation with resistivity.....	15
5.3	Comprehensive model of Þeistareykir geothermal field.....	16
6	Potential drilling targets	17
6.1	Earthquakes of 2014-2015.....	17
6.2	Resistivity anomalies surrounding the reservoir	17
6.3	Reservoir parameters, open fractures, and stress fields	18
6.4	Selected drilling targets.....	19
7	Summary and concluding remarks.....	19
8	References.....	22

List of Figures

Figure 1.	<i>Regional geological context.</i>	26
Figure 2.	<i>Recall of main the results from phases 1 and 2 (1)</i>	27
Figure 3.	<i>Recall of some results from Phases 1 and 2 (2).....</i>	28
Figure 4.	<i>Recall of some results from Phases 1 and 2 (3).....</i>	29
Figure 5.	<i>Recall of some results from Phases 1 and 2 (4).....</i>	30
Figure 6.	<i>Previous structural targets intended by drilling and findings in Þeistareykir wells</i>	31
Figure 7.	<i>Basic parameters used for the structural analysis of fractures and feeders</i>	32
Figure 8.	<i>Feeders and potential permeable fractures (1)</i>	33
Figure 9.	<i>Feeders and potential permeable fractures (2)</i>	34
Figure 10.	<i>Feeders and geometry of potential permeable fractures at depth (1).....</i>	35
Figure 11.	<i>Feeders and geometry of potential permeable fractures at depth (2).....</i>	36
Figure 12.	<i>Provinces of formation temperatures.....</i>	37

Figure 13. <i>Changes in formation temperatures and potential structural control</i>	38
Figure 14. <i>Structural interpretation of suggested fractures in formation temperatures in terms of the shift of Þeistareykir fissure swarm on the WNW Stórhver-Bæjarfjall dextral Fault</i>	39
Figure 15. <i>Compilation of the relevant multidisciplinary structural data, excluding the resistivity</i>	40
Figure 16. <i>Compilation of the multidisciplinary structural data and lineations controlling the resistivity anomalies at 500 m b.s.l.</i>	41
Figure 17. <i>Compilation of the multidisciplinary structural data and lineations controlling the resistivity anomalies at 1000 m b.s.l.</i>	42
Figure 18. <i>Compilation of the multidisciplinary structural data and lineations controlling the resistivity anomalies at 1500 m b.s.l.</i>	43
Figure 19. <i>Compilation of the multidisciplinary structural data and lineations controlling the resistivity anomalies at 2000 m b.s.l.</i>	44
Figure 20. <i>Compilation of the multidisciplinary structural data and lineations controlling the resistivity anomalies at 2500 m b.s.l.</i>	45
Figure 21. <i>Compilation of the multidisciplinary structural data and lineations controlling the resistivity anomalies at 3000 m b.s.l.</i>	46
Figure 22. <i>Compilation of the multidisciplinary structural data and lineations controlling the resistivity anomalies at 4000 m b.s.l.</i>	47
Figure 23. <i>Compilation of the multidisciplinary structural data and lineations controlling the resistivity anomalies at 5000 m b.s.l.</i>	48
Figure 24. <i>Suggested areas and structural targets for drilling</i>	49

List of maps

Map 1. <i>Multidisciplinary structural model of Þeistareykir geothermal field, potential drilling targets, and fault geometry</i>

1 Introduction

From 2013 to 2015, ÍSOR undertook a geological re-evaluation of Þeistareykir and surroundings in three phases (Khodayar and Björnsson, 2013; Khodayar, 2014; Khodayar et al., 2015). The emphasis of the first two phases was to provide Landsvirkjun with an overview of the tectonics processes controlling the surface and sub-surface geology, including the geothermal activity. The ultimate goal is to suggest new targets for drilling based on the results of the three phases of the multidisciplinary structural analysis.

The preparatory works carried out during Phases 1 and 2 brought new insights into the regional and local tectonics of Þeistareykir such as:

- The fracture sets of rift and transform zones at Þeistareykir and surroundings from aerial images, and their preliminary statistical analysis.
- Correlation of the tectonic pattern with earthquakes and structural data from televiewer image logs in well ÞG-8.
- Tectonic control of surface alteration and gases.
- Tectonic settings of resistivity, aeromagnetic and gravity anomalies.
- The shift of the Þeistareykir fissure swarm on one of the transform zone faults.

This report presents the results of Phase 3 of the multidisciplinary geological exploration at Þeistareykir and surroundings, the synthesis of the results from the three phases, along with new areas and structural targets for drilling and exploration. As the geothermal field is at the junction of the Northern Rift Zone and the transform zone of Tjörnes, at any level it is subjected to deformation resulting from both types of plate boundaries (Figs. 1a and 1b).

The focus of Phase 3 is on the analysis of existing borehole data and their structural interpretation, as well as on the overall correlation and synthesis of the results obtained from the multidisciplinary geological exploration of all the three phases. The main topics of Phase 3 are:

- A brief review of existing structural interpretations of Þeistareykir and previous suggested structural targets for drillings.
- New structural analysis of feeders in the 10 Þeistareykir wells and identification of potential permeable fractures.
- Possible structural control of formation temperatures and feeders in wells, and their relation to the shift of the Þeistareykir fissure swarm.
- Correlation of all geophysical and geological sub-surface data with the structural map of rift and transform zones at Þeistareykir from Phases 1 and 2.
- Comprehensive structural model of the Þeistareykir geothermal field.
- Synthesis of the findings of the three phases.

The outcome of the above analysis and synthesis should provide Landsvirkjun with an in-depth view of how the tectonics of rift and transform zones control various aspects of geothermal activity in the Þeistareykir fractured reservoir. With a better understanding of the fracture sets, their depths, and their roles in fluid flow, alteration, and heat, we

hope to offer a comprehensive tool for the choice of new areas and structural targets for exploration and production drillings in Þeistareykir. The choice of these drilling targets is based on the most complete exploration effort to-date.

2 Geological settings

2.1 The general context

The Þeistareykir geothermal field is located within the Northern Rift Zone (NRZ), and between the Húsavík-Flatey Fault and the Dalvík Lineament of the Tjörnes Fracture Zone (TFZ) (Fig. 1a). Due to its position at the junction of a rift segment and a transform zone, the geothermal field has been in a highly deformed area where rift-jumps, flexuring, block rotation and intense fracturing occur since Miocene (e.g., Sæmundsson, 1978; Voight and Mamula, 1983; Jancin et al., 1985; Young et al., 1985; Garcia et al., 2002).

The known features of the plate boundaries are:

- *Rift fissure swarm*: Five parallel fissure swarms stretch within the 40 km width of the NRZ. The Þeistareykir and Mánáreyjar fissure swarm are the westernmost of these fissure swarms and are located partly on-land and partly offshore. Northerly normal faults and open fractures are dominant within the rift segments. Although numerous eruptive cones are aligned on fractures, very few northerly dykes crop out within the Þeistareykir fissure swarm and no apparent caldera is known at the surface. The bedrock of Þeistareykir and surroundings spans Miocene to interglacial/subglacial times (Bruhnes-Weischselian), and consists of basaltic, andesitic and dacitic lavas, hyaloclastites, local rhyolite, and the Pliocene marine fossil-rich Tjörnes formation. The postglacial basaltic lavas are younger than 15.000 years. They include the latest eruption of 2400 years ago, which emitted picrite from the Stórhver crater within the Þeistareykir fissure swarm (Sæmundsson et al., 2012a).
- *Transform zone*: The TFZ is considered to have been active at least since 6–7 Ma ago, with both subsidence in the order of hundreds of metres and a dextral shift of some 100 km (e.g., Sæmundsson, 1978). The transform zone is some 120 km long, about 70 km wide, consisting of three major WNW trending structures, i.e., the Grímsey Oblique Rift, the Húsavík-Flatey Fault (HFF) and the Dalvík Lineament (Fig. 1b). The HFF has an established fault plane where earthquakes occur on it offshore (Rögnvaldsson et al., 1998). The Dalvík Lineament has a sharp signature in the topography in its eastern part, but earthquakes are recorded mostly in the western part of this structure on north-easterly sinistral strike-slips to the north of the lineament (Stefánsson et al., 2008). GPS measurements (Geirsson et al., 2010) indicate continuous deformation of the TFZ, with earthquakes up to M7 (Einarsson and Björnsson, 1979). Focal mechanisms of earthquakes in the TFZ indicate strike-slip motions on northerly, NNE/NE, WNW and NW fracture segments (Rögnvaldsson et al., 1998), supported by relocated earthquakes at Þeistareykir (Hjaltadóttir and Vogfjörð, 2011).

Surface geological investigations in the adjacent Flateyjarskagi (Voight and Mamula, 1983; Young et al., 1985; Mamula and Voight, 1985), and Þeistareykir (Gíslason et al., 1984) also show the existence of several fracture sets at the junction of the rift and the transform zone. However, the geological maps of Þeistareykir and surroundings (Fig. 1c) favour dominantly the rift-parallel northerly normal faults and open fissures along with a few WNW fracture segments (e.g., Sæmundsson et al., 2012b).

2.2 Recall of the structural re-evaluation of Þeistareykir

More recent structural re-evaluations of Þeistareykir and surroundings from aerial images and subsurface (Khodayar and Björnsson, 2013; Khodayar, 2014; Khodayar et al., 2015) reflect the same tectonic pattern as in most previous works, in which six fracture sets belonging to the rift and transform zones are widespread. These new re-evaluations show the role of the six fracture sets in the overall deformation and the degree in which they control the geological processes and the geothermal activity. A quick overview of the results from Phases 1 and 2 is given below:

- About 10729 fracture segments of variable lengths were mapped from aerial images. They consist of the northerly rift-parallel fractures and five Riedel shears of the transform zone striking NNE, ENE, E-W, WNW and NW/NNW. Except for the discreet E-W set, the other Riedel shears are oblique-slips, with dextral (WNW, NW/NNW) and sinistral (NNE and ENE) motions based on their *en échelon* geometries. The six fracture sets are grouped in tightly parallel weak zones and spread throughout the region (Fig. 2b).
- The detailed statistical analysis of the fracture frequency vs. rock age reveals that the WNW, NNE, ENE, NW/NNW and E-W Riedel shears of the transform zone dominate in the 2400 year old lava in the middle of the Þeistareykir fissure swarm. As rocks become older, the northerly fractures are more prominent and more frequent on the shoulders of this fissure swarm where they constitute up to 10% of the total fracture population. Thus, the Riedel shear seems more dominant at the youngest stage of fracture formation. As an example, the last eruption in the central part of Þeistareykir fissure swarm (2400 years ago) occurred on a WNW dextral fracture segment stretching from Stórhver to Bæjarfjall (Khodayar et al., 2015). In fact, this WNW weak zone is also responsible for the dextral shift of Þeistareykir fissure swarm. Hence, the northerly central pull-apart structures and faults on each side of the WNW structure are not the same (Fig. 2c).
- The strike and motions of the six fracture sets at Þeistareykir and surroundings are compatible with the spreading direction of N105°E identified by DeMets et al. (2010) (Fig. 2b). They are also identical to the fracture sets identified from regional earthquakes in the TFZ (Fig. 1b) or locally around the geothermal field (Figs. 3a to 3d), and seen on televiewer image logs at depth in at least one well in the middle of the Þeistareykir fissure swarm (Figs. 3f to 3g).
- Locally and above the geothermal reservoir, the Riedel shears control the location and distribution of the alteration and gases (Figs. 4a to 4c). Regionally, the influence of the rift and transform zone fracture sets is also obvious in the aeromagnetic structures and gravity anomalies (Figs. 4d and 4e).

- The resistivity structures display striking *en échelon* arrangements indicative of dextral and sinistral motions along the WNW to NW/NNW, NNE, and ENE and Riedel shears almost at the same locations as the surface mapping indicate fractures of same strikes and motions. Only locally the resistivity structures reflect the influence of rift-parallel northerly lineaments (Khodayar et al., 2015).
- More importantly, the tectonic lineaments controlling the resistivity structures undergo a gradual clockwise rotation, up to 40°E, from 1000 to 4000 m b.s.l. (Figs. 5a and 5b), an anti-clock rotation of 4° to 16° W at 5000 and 6000 m b.s.l. (Fig. 5c), and again a clockwise rotation of 2° to 14° E at 8000 m b.s.l. (Fig. 5d). Riedel shears dominate the upper 6000 m in the crust, but at 8000 m b.s.l., few N-S, E-W, WNW and NNW lineaments equally control the tectonic configuration. The E-W lineaments are the deepest set of fracture appearing from 4000 m b.s.l., which explains why E-W fractures are so uncommon at the surface.
- The geometrical configuration of the resistivity structures reflects the strike-range of the fractures emerging from all other data (Fig. 5e). As a result of the rotation of the resistivity structures, the depths at which individual fracture sets seem most common appear to be of the outmost importance for drilling (Fig. 5f).

The results of Phases 1 and 2 are a major input in the analysis of Phase 3 since it relies heavily on them.

3 Previous drilling targets at Þeistareykir

Before proceeding to a new structural analysis of borehole data, results of previous choices of drilling targets as well as the outcome of the drillings at Þeistareykir are discussed.

The 10 deep high-temperature wells at Þeistareykir were drilled over a period of 11 years (2002 to 2012). From early stages of exploration and drilling (ÞG-1) up to the last well (ÞG-9), the drilling targets have been chosen based on surface alteration or chemical evidence, TEM-MT model, but most importantly on the northerly fractures of the rift (e.g., Guðmundsson et al., 2008; Mortensen, 2012). The exception to the northerly structural targets is the highly altered NW Tjarnarás Fault (Fig. 6a), which appears as an isolated structure unrelated to the rift.

The depth of the wells at Þeistareykir range from 1627m to 2659 m (TVD), thus reflecting the status of fracturing in the uppermost 2–2.5 km in the crust. We extracted from all borehole data available the indications of fracturing (Figs. 6b to 6d), be it ample alteration, mineral veins or intrusions, along with the depth ranges of feeders (Guðmundsson et al., 2002; Guðmundsson et al., 2004; Þórarinnsson et al., 2006; Richter et al., 2007; Blischke et al., 2007; Ingimarsdóttir et al., 2009; Árnadóttir et al., 2009; Árnadóttir et al., 2011; Nielsson et al., 2011; Blischke and Árnadóttir, 2012; Mortensen et al., 2013). Two points appear from the analysis of borehole data:

- The feeders are considered to be associated mostly with intrusions, which can be sills but also dykes (i.e., fractures) at depth. A portion of the feeders, however, is not associated with intrusions in which case they could likely be associated with permeable faults.

- Intervals of secondary fractures such as broken rock are frequently reported in all wells. They are either in association with mineral veins or alteration, i.e., more typical of faulting rather than intrusions. From the analysis of borehole data it appears that the fractured intervals at depth are much more frequent than the number of the northerly faults mapped at Þeistareykir, which were used as drilling targets. As a matter of fact, even a limited 300 m section logged with televiewer (1498–1773 m) in well ÞG-8 shows that the number of faults and the variety of strikes found at depth are more than those suspected from previous structural maps (Figs. 3a and 6a). Therefore, a re-interpretation of selected borehole data using our structural map is attempted below, as results could be rewarding.

4 New structural analysis of borehole data

For our structural analysis of borehole data, we used two sets of data from existing wells and interpret them using our structural map. One set is the feeders, and the other the formation temperatures recorded in all 10 Þeistareykir wells.

4.1 Feeders and fractures in existing wells

The summary of data that we prepared for the structural analysis of feeders and fractures is presented on Table 1. In order to compare which of our suggested fractures on the maps could coincide with the feeders at depth, we projected the point of intersection of the feeders in the wells onto the surface and along the well paths, and estimated their distances from well head. Respecting the dip direction of the fractures, we also calculated which structures surrounding individual wells could intersect the depths at which individual feeders are found in each well. The distance of those selected fractures from well heads is also reported on Table 1, except for vertical wells, where the depths of the feeders remain as points at the well heads. Finally, along with the strikes of the fractures, we also show the best dip values of the permeable fractures if they are to coincide with the specific depths of the feeders in each well.

Figures 7a, 7b, and 8a show the best permeable fractures matching the feeders of wells as grouped in three areas. On those figures, the circles representing the feeder and the matching fractures are shown in the same colour. About 5 faults could potentially match the feeders of ÞG-8 (Fig. 7a), 11 fractures the feeders of ÞG-1, ÞG-5, ÞG-5b, ÞG-2, and ÞG-4 (Fig. 7b), 12 fractures and one dyke the feeders of ÞG-3, ÞG-7, ÞG-6 and ÞG-9 (Fig. 8a). In many cases, however, more than one set of potential permeable fractures could match an individual feeder, in which case those fractures are marked as and/or on maps. A summary of all fractures and feeders is reported on figures 8b and the fractures numbered on figure 9a. The fault geometries, dips, and segmentations of these fractures and how they match the feeders are reported on figures 9b to 9m and 10a to 10n.

This structural analysis reveals four features regarding the potential permeable fractures:

- *Strikes*: The most frequent permeable fracture sets are the ENE and then northerly. However, in the group of possible permeable fractures, the northerly rift-parallel fractures are as frequent as the ENE sinistral and WNW dextral

oblique-slip Riedel shears of the transform zone (Fig. 8b). To reiterate, the existence and importance of the ENE fractures have been demonstrated both in our structural analysis of ÞG-8 and in the televiewer data of that well (Fig. 8a).

- *Dips:* All suggested permeable fractures match the corresponding feeders if those fractures dip $> 80^\circ$ (Table 1, Figs. 9 and 10). The dips seem to remain as such, regardless of the depth at which the feeders are found in the wells. These dip values are important since they indicate steeply-dipping fracture planes, which can be easily missed if their dip values are unaccounted for during drilling.
- *Segmentation:* Even with steep dips, the fracture planes must be segmented at depth in order to match the depths of specific feeders (Figs. 9b to 9m, 10b to 10n). This is not surprising since segmentation is already apparent from their surface geometries on all maps. Attempts were made to find the best structural matches for the feeders, respecting the dip value, dip direction, depth and the geometry of the fractures. However, the segmentations shown on figures are only indicative of fracture geometry since the exact number of segments along individual fracture at depth is in fact unknown.
- *Opposite dip directions:* As it appears from the surface, a fracture can consist of several segments along its trace. Due to their steep dips, fracture planes can present opposite dip directions. It is estimated that these features are shallow in the crust as the fractures coalesce into a single plane at greater crustal depths.

4.2 Formation temperature

The surface alteration at Þeistareykir and immediate surroundings (Fig. 11a) should somewhat be indicative of areas with elevated temperatures at depths. However, the analysis of formation temperatures indicates other configurations (Figs. 11b to 11e).

The formation temperatures of the 10 exploration/production wells fall clearly into three groups Figure 11b:

- Group (1) consisting of wells ÞG-2, ÞG-5, ÞG-5b, and ÞG-7: In this group, the temperature is inverted below 150–400 m b.s.l (TVD). The deepest of these wells, i.e., ÞG-5b, recovers to the boiling curve at below 2000 m b.s.l. (TVD).
- Group (2) or wells ÞG-1, ÞG-3, ÞG-4, ÞG-6 and ÞG-9: In this group, the temperature follows the boiling curve without any inversion.
- Group (3) or ÞG-8: This well attains a maximum of 210°C at 150 m b.s.l. (TVD), but is inverted from that depth down to the bottom of the well where the temperature is 110°C at 1850 m b.s.l (TVD) (ÍSOR database).

Alteration minerals found in the wells are generally in good accordance with the formation temperature except for well ÞG-8 where the alteration minerals indicate a former temperature of 250°C near the bottom of the well (Níelsson et al., 2011).

On figure 11c, the wells are coloured according to the group to which they belong. As each group occupies a specific area on the map, an extrapolation is made to identify larger areas that could be covered by the formation temperature of individual group. Figure 11d shows that the central part of Þeistareykir could fall under Group (2), while the areas on either sides of it correspond to Group (1).

The distribution of Group (2) can be interpreted as an up-flow zone in the central part of Þeistareykir, as it is the hottest and the well follows the boiling curve at depth. That of Group (1) can be seen as hot at shallow depth and colder at greater depth, and explained as outflow zones. Since Group (3) is located farthest from the centre of the reservoir, only the tip of the outflow zone reaches as far as ÞG-8 to the west thus warming up only the upper part of the well (Fig. 11e). The lower part of ÞG-8 is colder than the expected real formation temperature of the area to the west. The bottom temperature of 110° C at 2000 m (TVD) corresponds to a thermal gradient of only 55° C/km. The existence of an up-flow zone, not so far from our suggestion configuration, has been already pointed out by Gíslason et al. (1984) and Guðmundsson et al. (2008).

4.3 Structural provinces of formation temperatures

To assess whether there could be a structural control of formation temperatures, we identified on temperature logs the depths at which the uppermost break in the formation temperature occur (Figs. 12a and 12b). We then projected those depths to the surface along the well paths (Fig. 12c). Finally, we attempted to find the best possible fractures that cross those points and could explain the changes in the heat.

Two scenarios can be envisaged. One is considering only the rift-parallel faults, and the other is a combination of rift and transform zones fracture sets. These are described below:

- Only the rift-parallel faults are considered, as the northerly fractures have been the favourite structural targets for drilling. The four best matches are numbered as 1 to 4 on figure 12d. Of these, Faults 1 and 2 could be those that fall between the outflow zone and the area of Group (3) where ÞG-8 is located. In that case, this could be a boundary fault compartmentalising the area of Group (3) from the reservoir, thus explaining the colder temperatures at depth in ÞG-8. Fault 3 could separate the areas of Group (1) and (2) and cross the groups of wells sharply. Fault 4 at Ketilfjall is the eastern boundary structure of the Þeistareykir fissure swarm. Since it dips to the west, it could potentially cross ÞG-7 at the depth where the change in formation temperature occurs.
- Both the northerly rift-parallel fractures and the Riedel shears of the transform zone are considered (Fig. 12e). Two of the 10 suggested structures are the same northerly segments as in scenario one that could potentially separate Group (3) from Groups (1) and (2). They are labelled as 1 and 2 here. The 8 other Riedel shears, labelled as segments 3 to 10, are those that fit best with the changes in formation temperatures, although the configuration of the formation temperature is unknown farther away from the reservoir.

The Riedel shears labelled as 3, 7, 8 and 9 strike WNW. Segment 3 could dip to the SW, similar to other WNW segments further to the north (Fig. 12e). Due to its steep dip, this segment coincides with the point where the formation temperature changes in ÞG-7 from the boiling curve (shallower up-flow zone from the reservoir) to cooler temperature at depth (Figs. 11e, 12b and 12e). The WNW segment 7 acts as the best boundary between the up-flow zone and the cooler formation temperatures of Groups (1) and (2). Segment 8 is highlighted since it forms with segment 7 the major dextral oblique-slip fault on which the eruption

of Stórhver as well as the changes in alteration and possibly the formation temperature occur. The role of segment 9 in the geothermal reservoir is unknown because of lack of data around this segment. But if the boundary of Group (1) lies, as shown, to the southwest of ÞG-2, then this WNW segment is the best candidate. Of the three other ENE structures, segment 4 is the best match to divide the Groups (1) and (2) crossing right between ÞG-5/ÞG-5b and ÞG-1/ÞG-4. It could also be the boundary of the up-flow zone to the east. Segment 5 limit the up-flow zone and outflow zone to the west/northwest. The point of change in formation temperature in ÞG-8 could be on the WNW segment 6 (found strongly in the televiewer data), as much as on the NW segment 10 (Fig. 12e).

The favourable structures of each scenario, however, must be considered taking into account the regional geological context that controls the geothermal processes. If the suggested structures are interpreted in view of the shift at Þeistareykir, it appears clearly that the northerly structures 1, 3, and 4 to the north (Fig. 13a) do not cross the WNW splay segment of the dextral strike-slip Stórhver-Bæjarfjall Fault and, therefore, segment 2 to the south is not their continuation. It is thus unlikely that the northerly segments divide the wells of Group (1) from Group (2) and play a significant role in the changes in the formation temperatures there. On the other hand, the ENE and WNW Riedel shears seem better matching with the shift of Þeistareykir as some of the suggested WNW segments are the same as the segments of the Stórhver-Bæjarfjall Fault (Fig. 13b). Additionally, the ENE segments seem to better compartmentalise the provinces in the formation temperatures. It is noticeable that the Riedel shears suggested in scenario 2, are identical to those controlling the feeders, and in a few cases they are the same segments.

The analysis of formation temperatures and the correlation with the feeders supports the fact that the Riedel shears of the transform zone play a critical role in fluid flow and geothermal processes altogether.

5 Multidisciplinary data correlation and modelling

In the following chapters, we compile all the results from the analysis of various datasets obtained during Phases 1, 2 and 3. This compilation gives an overview of the most active structures in the geological processes leading to geothermal activity. They are then used as the basis for suggesting the structural targets for drilling.

5.1 Correlation of borehole data with results of Phases 1 and 2

A number of structures emerge in the following parameters, which do not include the resistivity data (Fig. 14a):

- Formation temperature
- Feeders
- Surface alteration
- Earthquakes
- Gases
- Televiewer image logs.

The structures consist of major boundaries and, comparatively, secondary fractures. Some of the structures appear only in one set of data, but others are common to a series of processes. Despite their importance in regional tectonic, the two fault segments that act as the eastern boundary of the Þeistareykir fissure swarm show up in few data sets. As an example, the northerly fault of Ketilfjall appears in formation temperatures and acts as the boundary of the alteration block, the adjacent northerly dyke segments play a potential role among feeders in ÞG-7, but the Bóndhóll Fault appears only controlling a portion of the alteration block (Figs. 14a and 14b).

Other northerly normal and major NNE sinistral oblique-slip faults appear in formation temperatures, earthquakes, gases, and the alteration block to the west and southwest of Bæjarfjall. However, most of the major structural boundaries are the Riedel shears, including the NW striking Tjarnarás Fault. They control the feeders, the earthquakes, gases and bounding the alteration block at the surface. A series of ENE fractures stretching from the southern part of Tjarnarás Fault to the north of the crater in Bæjarfjall appear also among these same four datasets. Two main WNW dextral oblique-slip structures, i.e., the Stórhver-Bæjarfjall Fault and the fault between Tjarnarás and Ketilfjall appear in all dataset except the televiewer data.

The comparatively, “minor structures” striking ENE form a wide fault zone at ÞG-8 where at least 3 parallel faults are responsible for the broken zones and permeability associated with major feeders in that well. Potentially, a NW fault parallel to Tjarnarás could also play a role in that well, as well as in formation temperature (Fig. 14a). Other Riedel shears and a few short northerly segments, appear among one to two datasets (Fig. 14a).

The role of the major boundaries and secondary structures pops up better by compiling the outline of surface alteration, formation temperature, and the totality of the fracture pattern described above (Fig. 14b).

This present analysis reflects that the Riedel shears and the northerly rift-parallel fractures play an equal role in the surface and sub-surface geological processes. Their interaction leads to the compartmentalisation that appears in the configuration of the geothermal field in the upper 2 km crustal depth.

5.2 Further correlation with resistivity

The last data set to be compared in more detail with the above results is the tectonic control of the resistivity structures. For that correlation, we reported the potential structures that appeared controlling the resistivity structures at various depths, as they were analysed in Phase 2 (Khodayar et al., 2015).

The depth of the wells is within the uppermost 3 km of the crust. Therefore, we correlate the structures that match with the resistivity in the upper 5 km in the crust since the secondary fractures associated with the main structures between 3 and 5 km could still be present upwards in the shallower crustal depths (Fig. 5f) and be met during drilling.

Due to the rotation of the fractures controlling the resistivity structures at various depths, we correlate the lineations controlling the resistivity anomalies and our structural pattern at each individual depth. Figures 15a, 16a, 17a, 18a, 19a, 20a, 21a and

22a show the lineations controlling the resistivity structures, respectively, at the depths of 500 m, 1000 m, 1500 m, 2000 m, 2500 m, 3000 m, 4000 m, and 5000 m b.s.l. The lineations are directly reported on the structural map that reflects the six other datasets analysed above (Fig. 14a). On those figures, the individual fractures that match each lineation are numbered separately in each crustal depth. For clarity, only the lineations from resistivity and their counterparts from the analysis of other datasets are reported on figures 15b, 16b, 17b, 18b, 19b, 20b, 21b and 22b.

With all uncertainties when large sets of data are compared, a relatively good correlation appears between the lineation controlling the resistivity structures and the fractures observed in the six other data sets. In some cases, the Riedel shears and northerly fractures are exactly the same as the lineations seen in resistivity. In other cases, the lineations from resistivity fill the gap between segments that were already identified through formation temperatures, feeders, alteration block, earthquakes, gases and fractures identified on televiewer images.

The multidisciplinary data correlation with resistivity shows the same tectonic pattern as in other data sets, i.e., that the fracture sets of rift and transform zones together shape the geological processes at surface and depth.

5.3 Comprehensive model of Peistareykir geothermal field

The critical structures controlling the alteration block, formation temperatures, and all secondary permeable fractures are reported on a single map (Map 1a). Also shown are the lineations seen in resistivity. As that single model is to reflect the totality of the critical structures, the lineations controlling the resistivity structures are combined together regardless of their depths, and are all reported on the same map. The thickness of the blue lines summarises the segments of a particular weak zone that appeared at various depth intervals in the resistivity data.

This data compilation reflects a coherent structural model where the Riedel shears of the transform zones and the northerly rift-parallel fractures play a role in any process and at any depth.

The major boundaries stemming from this model are the boundaries of the alteration block and formation temperatures, not least the Stórhver-Bæjarfjall Fault where the splay segment of that fault is the most active segment above the reservoir (Map 1a). These boundaries are all Riedel shears of the transform zones where the ENE sinistral oblique-slip, the WNW and NW dextral oblique-slip faults dominate. These Riedel shears, along with a few of the northerly fractures are responsible for a complex structural compartmentalisation of the geothermal field. The secondary fractures of the same sets are the favourable structures controlling various parameters of the geothermal fractured reservoir.

As indicated from the analysis of resistivity, the WNW set is most frequent in the upper 2 km crustal depth, and again from 5 to 8 km depth. The ENE and NNW sets are more frequent between 2.5 and 5 km depths (Fig. 5f). Although the main weak zones of each set appear in a favourite depth, some fracture segments belonging to all sets could be secondarily spread throughout the upper 8 km crustal depths.

6 Potential drilling targets

In order to suggest new potential drilling targets, we considered in more detail several parameters such as (Map 1a to 1h):

- Resistivity anomalies
- Alteration block and formation temperatures
- Stress field
- Productivity index
- Fault geometry

6.1 Earthquakes of 2014–2015

While Phase 3 of the multidisciplinary structural analysis of Peistareykir was ongoing, new earthquake data were collected by ÍSOR for Landsvirkjun from late 2014 to 2015. The main bulk of these events is located to the west and northwest of the biggest crater in Bæjarfjall. As the earthquake data are not fully processed in time to be analysed and correlated from the beginning with all other data in our investigation, the 2014–2015 earthquakes are thus not included here.

However, an observation can be made. The last natural micro-earthquakes near the geothermal reservoir occurred between 1993 and 2011, and were located on the western slope of Bæjarfjall (Hjaltadóttir and Vogfjörð, 2011). The considerable 2014–2015 micro-earthquakes activity recorded by the ÍSOR-Landsvirkjun seismic network is farther to the east. Most of these events are to the west and northwest of the biggest crater of Bæjarfjall, and near the path of PG-4. From October 2014 to June 2015, all wells at Peistareykir, except PG-2, PG-5, and PG-8, were discharged (Júlíusson, 2015). It is, therefore, unclear how many of these earthquakes are related to the discharge and testing of geothermal wells, and how many of them result indeed from the natural release of the stress accumulated in the crust. It is likely that when fully processed, the fracture pattern suggested from our structural analysis appears also in the seismic lineations and fault plane solutions of the 2014–2015 events, and that the earthquakes appear mostly triggered by geothermal operation.

6.2 Resistivity anomalies surrounding the reservoir

We selected 5 resistivity cross-sections along NS (Map 1b) and EW lines (Map 1c) to check where the most obvious resistivity anomalies cross the reservoir and the targeted areas for drilling.

As their locations on the structural model of Peistareykir show, the anomalies (A), (D), and the northern part of (B) are beyond the main investigated area, where we did the least structural analysis due to low data density. Anomaly (C) to the west covers a part of the alteration block and the Group (1) wells. The southern part of anomaly (B) extends into the investigated area and coincides with the up-flow zone.

Of the resistivity anomalies along the EW lines, anomaly (H) and only a part of anomalies (E) and (F) coincide with parts of the alteration block and with some of the structural compartments seen in formation temperatures. Note that (F) and (H) are

sections through the same resistivity anomaly. Almost half of these anomalies fall also outside of the reservoir area in regions where other data density is low.

Therefore, in our suggestions of structural targets, we focus mostly on areas that cover both the resistivity anomalies and our thorough structural model.

6.3 Reservoir parameters, open fractures, and stress fields

The fracture sets that play a critical role in the compartmentalisation of the formation temperatures, and create permeability for the feeders are mostly the same as bounding the alteration block at the surface (Map 1d). These fractures are a combination of rift and transform structures. They are dominantly the ENE sinistral and the WNW dextral oblique-slip faults, including the splay segments of the Stórhver-Bæjarfjall Fault stretching to the geothermal reservoir. Furthermore, a few NW dextral oblique-slip segments, particularly the Tjarnarás Fault and the segment to its west are the most important structures. The northerly set consists of shorter segments, however.

The main boundaries represented on Map 1d could, however, change if more borehole data become available beyond the alteration block.

The fractures compartmentalising the reservoir are all open fractures. The rift-parallel fractures are by nature extensional structures, but the Riedel shears are also open since they have a dip-slip component.

The fact that all fracture sets are open is supported also by the regional and local stress fields at and within the rift and transforms plate boundaries (Maps 1e). Although the overall spreading direction is at N105°E (DeMets et al. (2010), in more details, fluctuations are suggested across the rift and transform segments in North Iceland and offshore (Map 1e). The spreading direction is nearly N102°E near the rift segments but is oriented ~ N80° E across the TFZ but the total displacement is broken up in transversal and lateral displacements resulting in strike and dip-slip motion of the transform fault segments (Garcia et al., 2002). The field structural analysis of kinematic indicators between the Húsavík-Flatey Fault and Dalvík Lineament shows complex sets of stress fields to be responsible for normal and strike-slip faulting (Homberg et al., 2010). According to this analysis, a large area to the western part of the transform zone is subject to severe fluctuations in the direction of SH_{max} (Map 1e), resulting in all fracture sets being potentially open. That analysis, however, does not take into account block rotation.

Peistareykir is farther east compared to the areas under structural investigations by Garcia et al. (2002) and Homberg et al. (2010). As the geothermal field and its surroundings are also between the Húsavík-Flatey Fault and Dalvík Lineament, the same sets of stress fields as the western part of the transform zone are likely applicable to the fracture sets of Peistareykir.

The production capacity of wells at Peistareykir, as newly estimated by Júlíusson (2015) (Table 2), is reported and combined with the selected open fractures relevant to geothermal activity (Map 1f). Wells ÞG-2 and ÞG-8 are not producers. The wells ÞG-04 and ÞG-5B are with the highest production capacities, ÞG-1, ÞG-3, ÞG-6 with medium, and ÞG-7 and ÞG-9 have the lowest capacities of producing wells. From these

distributions, the best production capacity appears to the central and possibly southern part of the reservoir, bounded by the two WNW segments that form the splay of the Stórhver-Bæjarfjall Fault. It is unknown, however, if the production capacities are controlled by faulting alone, or by a combination of faulting and natures of displaced rocks where secondary minerals have not yet filled the pores and fractures.

6.4 Selected drilling targets

The ultimate goal of our three multidisciplinary phases of structural analyses has been to provide Landsvirkjun with an updated overview of the tectonic controlling the geothermal activity along with targets for drilling. Based on all results presented here, we suggest two types of drilling targets: Areas and structures.

- *Areas.* We identified five areas and ranked them in order of priority and according to the purpose of drilling (Fig. 23a). These areas are bounded by relevant tectonic boundaries and secondary structures. Area (A) is the most promising zone to be drilled as that area coincides with the up-flow zone from the reservoir. Drilling in that area is thus on the safe side and should provide the energy sought for the first stage of the power plant. Areas (B), (C), (D) and (E) are suggested as exploration areas where new wells would provide additional information on the size of the reservoir and the up-flow zone, as well as the permeability at depth. Of the exploration areas, areas (B) and (C) are with some basic information (i.e., resistivity and structural pattern), but both are outside of the alteration block with little gas measurements for hints on host fractures. Areas (D) and (E) are with least data and are thus riskier. However, drilling into the four zones should be equally important as Landsvirkjun may need to expand its operation beyond the limited area drilled up to the present.
- *Structural targets.* Within each of the five areas, we highlighted the favourable potential structural targets, which stem from our multidisciplinary structural analyses. These structural targets are shown on figure 23b, and are: (a) Fault intersections, which would provide the best permeability; (b) A few WNW, ENE and northerly segments where drilling could be carried out along the fracture trace. The majority of the structural targets has not been intersected by previous drillings at Þeistareykir.

Finally, when designing the drill paths, particular attention must be paid to fault geometries, segmentations, and the dip of the fracture planes. Although all fracture sets could be potentially open, due to their steep dip and segmentations, the structural target may not be reached by drilling at the intended location and depth (Maps 1g and 1h).

7 Summary and concluding remarks

In this last phase of our structural analysis, we: (a) Evaluated the previous drilling targets; (b) Examined the permeable fractures that could potentially be the paths for feeders found in wells; (c) Investigated the formation temperatures and their possible structural control; (d) Correlated results of all surface and sub-surface data obtained during the three phases; (e) Suggested new drillings targets at Þeistareykir.

The highlights of our results are:

- Except for chemical and alteration indications, a few northerly fractures have been the favourable choice of structural targets for the drilling of wells ÞG-1 to ÞG-9. However, the re-evaluation of borehole data indicates that there are more broken areas at depth associated with fracturing and intrusions than the few northerly fractures at and surrounding Bæjarfjall.
- The analysis of feeders with our structural pattern of rift and transform zones shows that the dextral WNW and NW, as well as the sinistral ENE oblique-slip faults are the main permeable fractures along with a few of the northerly shorter segments.
- The structural boundaries controlling the alteration block at the surface, along with the associated parallel fractures through which gases and feeders seep are the same sets as those that control the formation temperatures and shape the boundaries of resistivity anomalies above the geothermal reservoir.
- Among the main boundaries, the splay section of the WNW Stórhver-Bæjarfjall dextral fault enters the reservoir. Due to the dextral shift along this fault that displaces the entire Þeistareykir fissure swarm in the middle, the northerly short segments to the north and south of this fault are not the same.
- The analysis of the varied surface and sub-surface data shows that the Riedel shears of the transform zone play an important role in the geological processes controlling the geothermal activity.
- Using the combined structural pattern of rift and transform zone, we suggest drilling targets in terms of areas and structures. Of the 5 areas selected as drilling targets, the central zone mostly covers the up-flow zone of the reservoir. That zone is the safest area for additional production wells. The other four areas surrounding the central zone are exploration areas, which should provide further information about the extent of the reservoir and its characteristics. Within each of these five areas, a number of permeable structural targets are suggested that could tap into the best reservoir temperatures. These structural targets are either fracture intersections between Riedel shears and/or northerly rift-parallel fractures, or fracture traces. They are, however, mostly the Riedel shears of the transform zone.
- As the earthquakes of 2014–2015 coincide in time mostly with the period when the wells in Þeistareykir were discharged, it is likely that many of those events are a response to the geothermal operation rather than reflecting the natural release of stress along faults. These events appear to have occurred to the west and northwest of the biggest crater in Bæjarfjall, near the path of ÞG-4. Their location coincides with a large part of the main target area for drilling and a number of selected fractures there, but also with one of the areas selected for exploration drilling.

Three points should be emphasised:

1. The data regarding the micro-earthquakes of 2014–2015 recorded by the ÍSOR - Landsvirkjun seismic network were not fully processed at the time of our investigations in order to be included in our structural analyses and be correlated with all other data sets. It is recommended that a side project is allocated to correlate the seismic lineations and fault plane solutions emerging from the data processing of the 2014–2015 earthquakes with the results of our structural analysis, as it is likely that our suggested fracture pattern of rift and transform zones emerges also among the fully processed earthquake data.
2. When designing for new well paths, it is important to consider in details the features of the fractures. As the fractures are steeply-dipping and segmented, the drilling may not intersect the intended structure if their features are not taken into account accurately. Therefore, further work is required to evaluate the fractures and the drill paths.
3. Finally, a part of our structural analysis during the three phases of the multidisciplinary investigations uses available data up to date. If the base data regarding the formation temperatures, borehole data, and gas measurements change, our structural model of the Þeistareykir should be revised.

Acknowledgments. This report is prepared for Landsvirkjun. Our special thanks go to Ásgrímur Guðmundsson and Egill Júlíusson at Landsvirkjun for their support and project management. At ÍSOR, we wish to thank Sigvaldi Thordarson for his constructive review of this report; Steinþór Níelsson and Sveinborg H. Gunnarsdóttir for their help with Petrel in preparing the figures 9b to 9m and 10b to 10n; as well as Hrafnhildur Harðardóttir for editing this report.

8 References

- Árnadóttir, S., Ingimarsdóttir, A., Gautason, B., Mortensen, A. K., Egilson, P., Jónsson, R. B., Sveinbjörnsson, S., Tryggvason, H., and Vilhjálmsson, S. (2009). *Þeistareykir – Hola ÞG-6. 3. áfangi: Jarðlagagreining og mælingar*. Iceland GeoSurvey, ÍSOR-2009/072, 65 p.
- Árnadóttir, S., Egilson, P., Mortensen, A. K., Jónsson, S. S., Tryggvason, H., Ingólfsson, H., Vilhjálmsson, S., Kristinsson, B., Stefánsson, H. Ö., and Sveinbjörnsson, S. (2011). *Þeistareykir – Hola ÞG-7, 3. áfangi: Jarðlög og mælingar Borun vinnsluhluta fyrir 7" götuðum leiðara frá 776 m í 2509 m dýpi*. Iceland GeoSurvey, ÍSOR-2011/063, 87 p.
- Blischke, B., Gunnarsson, H. S., Gautason, B., Jónsson, S. S., Richter, B., Egilson, P., Kjartansson, O. Ó., and Jónsson, R. B. (2007). *Rannsóknarborun á Þeistareykjum – Hola ÞG-5. 3. áfangi: Borun vinnsluhluta frá 848 m í 1910 m*. Iceland GeoSurvey, ÍSOR-2007/056, 75 p.
- Blischke, A., and Árnadóttir, S. (2012). *ÞG-8 Televiewer and Composite Log Data Analysis: ABI-43 Acoustic Borehole Image and Lithology Log Data Processing and Interpretations for Depth Interval 1493.5–1775 m*. Iceland GeoSurvey, ÍSOR-2012/020, 43 p + 2 Appendices.
- DeMets, C., Gordon, R. G., and Argus, D. F. (2010). Geologically current plate motions. *Geophysical Journal International*, 181 (1), 1–80.
- Einarsson, P. (1979). Seismicity and earthquake focal mechanisms along the mid-Atlantic plate boundary between Iceland and the Azores. *Tectonophysics*, 55, 127–153.
- Einarsson, P. (1991). Earthquakes and present-day tectonism in Iceland. *Tectonophysics*, 189, 261–279.
- Einarsson, P., and Björnsson, S. (1979). Earthquakes in Iceland. *Jökull*, 29, 37–43.
- Garcia, S., Angelier, J., Bergerat, F., and Homberg, C. (2002). Tectonic analysis of an oceanic transform fault zone based on fault-slip data and earthquake focal mechanisms: The Húsavík-Flatey Fault zone, Iceland. *Tectonophysics*, 344, 157–174.
- Geirsson, H., Árnadóttir, Th., Hreinsdóttir, S., Decriem, J., LaFemina, P. C., Jónsson, S., Bennett, R. A., Metzger, S., Holland, A., Sturkell, E., Villemin, T., Völksen, C., Sigmundsson, F., Einarsson, P., Roberts, M. J., and Sveinbjörnsson, H. (2010). Overview of results from continuous GPS observations in Iceland from 1995 to 2010. *Jökull*, 60, 3–22.
- Guðmundsson, Á., Gautason, B., Thordarson, S., Egilson, P., and Þórisson, S. (2002). *Rannsóknarborun á Þeistareykjum Hola ÞG-01, 3. áfangi: Borun vinnsluhluta í 1953 m dýpi*. National Energy Authority, OS-2002/079, 59 p.
- Guðmundsson, Á., Gautason, B., Björnsson, G., Egilson, P., and Þórisson, S. (2004). *Rannsóknarborun á Þeistareykjum – Hola ÞG-2. 3. áfangi: Borun vinnsluhluta í 1723 m dýpi*. Iceland GeoSurvey, ÍSOR-2004/034, 56 p.

- Guðmundsson, Á., Gautason, B., Lacasse, Ch., Axelsson, G., Þorgilsson, G., Ármannsson, H., Tulinius, H., Sæmundsson, K., Karlsdóttir, R., Kjarran, S. P., Pálmarrsson, S. Ó., Halldórsdóttir, S., and Egilson, Þ. (2008). *Hugmyndalíkan jarðhitakerfisins á Þeistareykjum og jarðvarmamat með rúmmálsaðferð*. Iceland GeoSurvey, ÍSOR-2008/024, MV-049 Vatnaskil 08.05, 67 p.
- Gíslason, G., Johnsen, G. V., Ármannsson, H., Torfason, H., and Árnason, K. (1984). *Þeistareykir: Yfirborðsrannsóknir á háhitavæðinu*. National Energy Authority, report, OS-84089/JHD-16, 134 p., and 3 maps.
- Halldórsson, P. (2005). *Jarðskjálftavirkni á Norðurlandi - Earthquake activity in N-Iceland*. Veðurstofa Íslands, IMO report 05021, 34 p.
- Hjaltadóttir, S., and Vogfjörð, K. (2011). *Sprungukortlagning við Þeistareyki og Bjarnarflag með háupplausnarstaðsetningum smáskjálfta*. Landsvirkjun, report, LV-2011-116, 44 p.
- Homberg, C., Bergerat, F., Angelier, J., and Garcia, S. (2010). Fault interaction and stresses along broad oceanic transform zone: Tjörnes Fracture Zone, North Iceland. *TECTONICS*, VOL. 29, TC1002, doi:10.1029/2008TC002415, 12 p.
- Ingimarsdóttir, A., Egilson, Þ., Gautason, B., Sigurgeirsson, M. Á., Jónsson, R. B., Pétursson, F., Sveinbjörnsson, S., Sveinbjörnsson, S., Tryggvason, H. H., Jónsson, P., and Haraldsson, K. (2009). *Þeistareykir – Hóla ÞG-5b. Borun nýs vinnsluhluta út úr holu ÞG-5 frá 813 m í 2499 m dýpi. Jarðlagagreining og mælingar*. Iceland GeoSurvey, ÍSOR-2009/056, 43 p.
- Jakobsdóttir, S. S. (2008). Seismicity in Iceland: 1994–2007. *Jökull*, 58, 75–100.
- Jancin, M., Young, K. D., Voight, B., Aronson, J. L., and Sæmundsson, K. (1985). Stratigraphy and K/Ar ages across the west flank of the Northeast Iceland axial rift zone, in relation to the 7 Ma volcano-tectonic reorganization of Iceland. *Journal of Geophysical Research*, 90, 9961–9985.
- Júlíusson, E. (2015). *Álagsprófun á Þeistareykjum 2014-2015*. Landsvirkjun, short report 2014-403/08.02.04, 5 p.
- Khodayar, M. (2014). *Shift of Þeistareykir fissure swarm in Tjörnes Fracture Zone: Case of pull-apart on strike-slip?* Iceland GeoSurvey, report ÍSOR-2014/074, LV-2014-144, 21 p.
- Khodayar, M., and Björnsson, S. (2013). *Preliminary Fracture Analysis of Þeistareykir geothermal field and surroundings, Northern Rift Zone and Tjörnes Fracture Zone*. Iceland GeoSurvey, ÍSOR-2013/029. 57 p., 2 maps.
- Khodayar, M., Björnsson, S., Karlsdóttir, R., Ágústsson, K., and Ólafsson, M. (2015). *Tectonic Control of Alteration, Gases, Resistivity, Magnetism and Gravity in Þeistareykir Area. Implications for Northern Rift Zone and Tjörnes Fracture Zone*. Iceland GeoSurvey, report ÍSOR-2015/002, LV-2015-039, 59 p., 2 maps.
- Mamula, N., and Voight, B. (1985). Tectonic analysis of lineaments near spreading axis, Northeastern Iceland. *Tectonophysics*, 116, 63–93.
- Metzger, S., Jónsson, S., and Geirsson, H. (2011). Locking depth and slip-rate of the Húsavík-Flatey fault, North Iceland, derived from continuous GPS data 2006–2010. *Geophysical Journal International*, 187, 564–576.

- Mortensen, A. K. (2012). *Peistareykir. Tillögur um staðsetningu borholna í jarðhitakerfinu á Peistareykjum 2012*. Iceland GeoSurvey, ÍSOR-2012/043, 36 p.
- Mortensen, A. K., Egilson, P., Tryggvason, H., Kristinsson, B., and Vilhjálmsón, S. (2013). *Peistareykir – Hola ÞG-9. 3. áfangi: Jarðlög og mælingar. Borun vinnsluhluta fyrir 7" götuðum leiðara frá 828 m í 2194 m dýpi*. Iceland GeoSurvey, ÍSOR-2013/006, LV-2013-053, 78 p.
- Nielsson, S., Egilson, P., Gunnarsdóttir, S. H., Stefánsson, H. Ö., Jónasson, H., Tryggvason, H., and Vilhjálmsón, S. (2011). *Peistareykir – Hola ÞG-8, 3. áfangi: Jarðlög og mælingar. Borun vinnsluhluta með 8½" krónu frá 1495 m í 2503 m dýpi*. Iceland GeoSurvey, ÍSOR-2011/080, 67 p.
- Richter, B., Egilson, P., Mortensen, A. K., Jónsson, R. B., Thordarson, S., Pétursson, F., Kjartansson, O., Stacy, R., and Haraldsson, K. (2007). *Rannsóknarborun á Peistareykjum Hola ÞG-4 3. áfangi: Borun vinnsluhluta fyrir 7" leiðara frá 839 m í 2240 m dýpi*. Iceland GeoSurvey, ÍSOR-2007/054, 106 p.
- Rögnvaldsson, S. T., Gudmundsson, A., and Slunga, R. (1998). Seismotectonic analysis of the Tjörnes Fracture Zone, an active transform fault in north Iceland. *Journal of Geophysical Research*, 103, 30117–30129.
- Stefánsson, R., Guðmundsson, G. B., and Halldórsson, P. (2008). Tjörnes fracture zone. New and old seismic evidences for the link between the North Iceland rift zone and the Mid-Atlantic ridge. *Tectonophysics*, 447, 117–126.
- Sæmundsson, K. (1978). Fissure swarms and central volcanoes of the neovolcanic zones of Iceland. *Geological Journal, Special Issue*, 10, 415–432.
- Sæmundsson, K., Sigurgeirsson, M. Á., and Grönvold, K. (2012a). *Peistareykir. Jarðfræðirannsóknir 2011*. Iceland GeoSurvey, ÍSOR-2012/024, 61 p., with map.
- Sæmundsson, K., Hjartarson, Á., Kaldal, I., Sigurgeirsson, M. Á., Kristinsson, S. G., and Víkingsson, S. (2012b). *Geological Map of Northern Volcanic Zone, Iceland. Northern part. 1:100.000*. Reykjavík, Iceland GeoSurvey and Landsvirkjun.
- Voight, B., and Mamula, N. Jr. (1983). Structures and tectonics of northern Iceland. In J. E. Estes and G.A. (edits) *Thorley Manual of Remote Sensing, 2nd ed., Vol. 2.*, 1782–1786, American Society of Photogrammetry, Falls Church, Va.
- Young, K. D., Jancin, M., Voight, B., and Orkan, N. I. (1985). Transform deformation of Tertiary rocks along the Tjörnes Fracture Zone, North Central Iceland. *Journal of Geophysical Research*, 90, 9986–10,010.
- Þórarinsson, S. B., Guðmundsson, Á., Gautason, B., Egilson, P., Birgisson, K., and Sigurðsson, G. (2006). *Rannsóknarborun á Peistareykjum – Hola ÞG-3. 3. áfangi: Borun vinnsluhluta fyrir 7" leiðara frá 757 m í 2659 m dýpi*. Iceland GeoSurvey, ÍSOR-2006/053, 134 p.

Figures

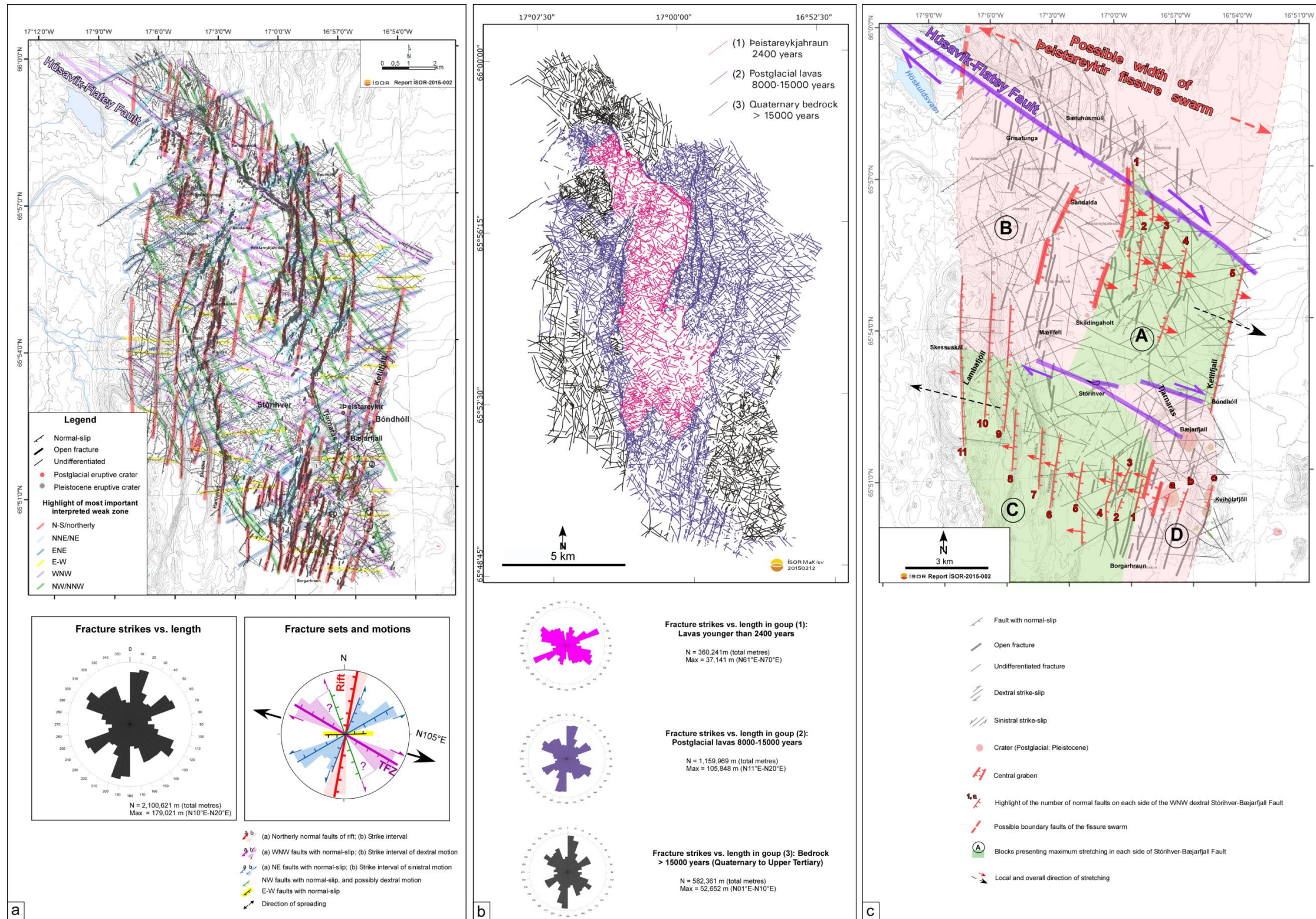


Figure 2. Recall of main the results from phases 1 and 2 (1). Main results regarding the fracture pattern. (a) Fracture pattern with highlights of the weakest zones along each of the six sets, the rose diagram of fracture frequency and the fracture motions. (b) Statistical analysis of the fracture population in terms of rock ages. (c) Number of normal faults on each side of the WNW Stórihver-Bæjarfjall Fault and the shift of the Peistareykir fissure swarm in a dextral motion along this fault.

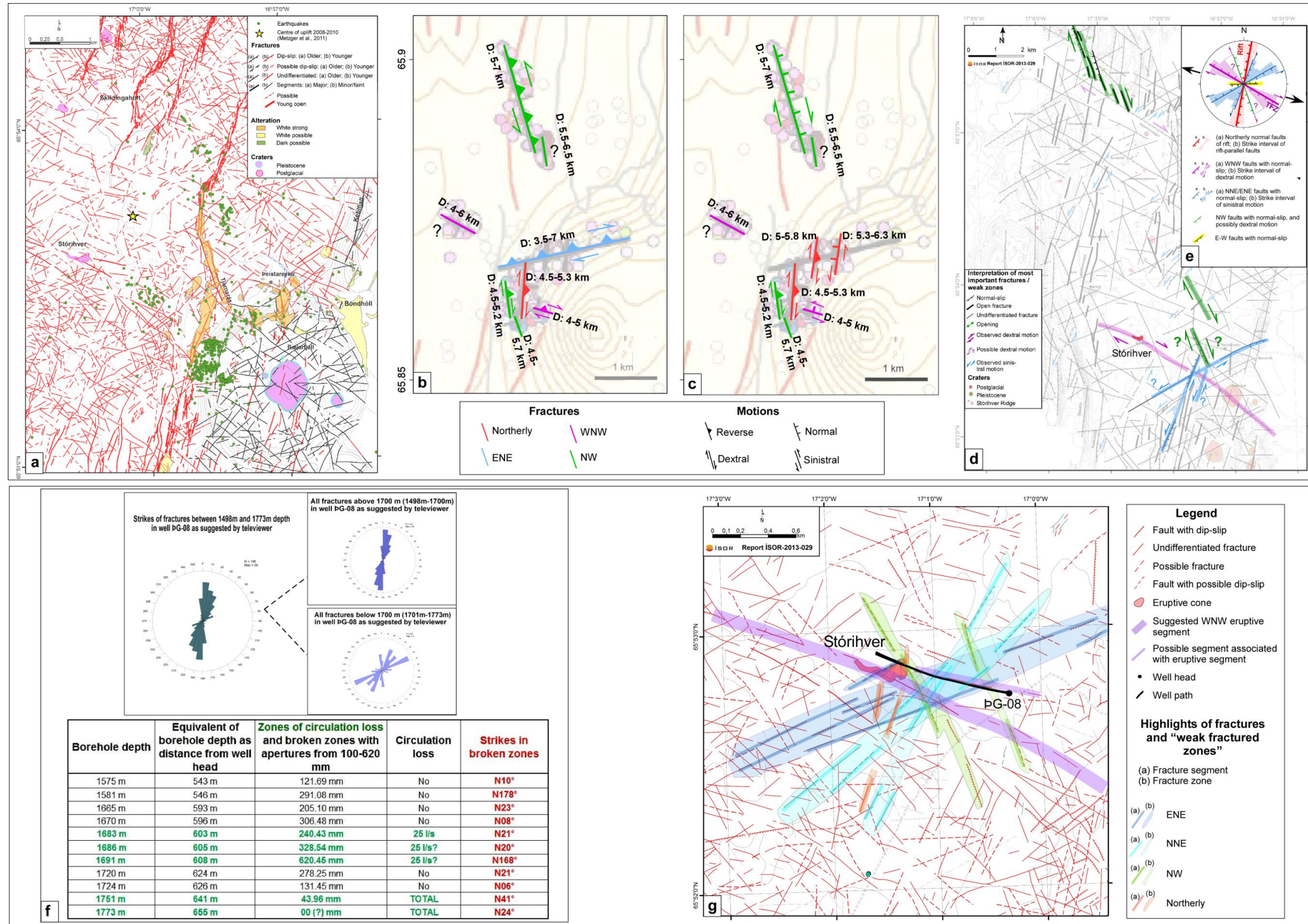


Figure 3. Recall of some results from Phases 1 and 2 (2). (a) The relocated earthquakes ($M -0.6$ to 3.2) from 1993 to 2011 (Hjaltadóttir and Vogfjörð, 2011), and the centre of uplift in Deistareykir. Metzger et al. (2011) reported on our raw structural map. (b) and (c) Four clusters of earthquakes along with two options for the interpretation of the strikes and motions of the corresponding faults (Hjaltadóttir and Vogfjörð, 2011). (d) and (e) Correlation of our fracture pattern with relocated earthquakes from 1993 to 2011, and significance of the fracture pattern. (f) Strikes of all fractures interpreted from televiewer image logs between 1498 m and 173 m depth, their subdivision above and below 1700 m, along with the table of the widest broken zones and circulation losses at those depths (Blichke and Árnadóttir, 2012). (g) The fractured zones comprising the suggested fracture segments that intersect the well and coincide with the structures seen in the televiewer data.

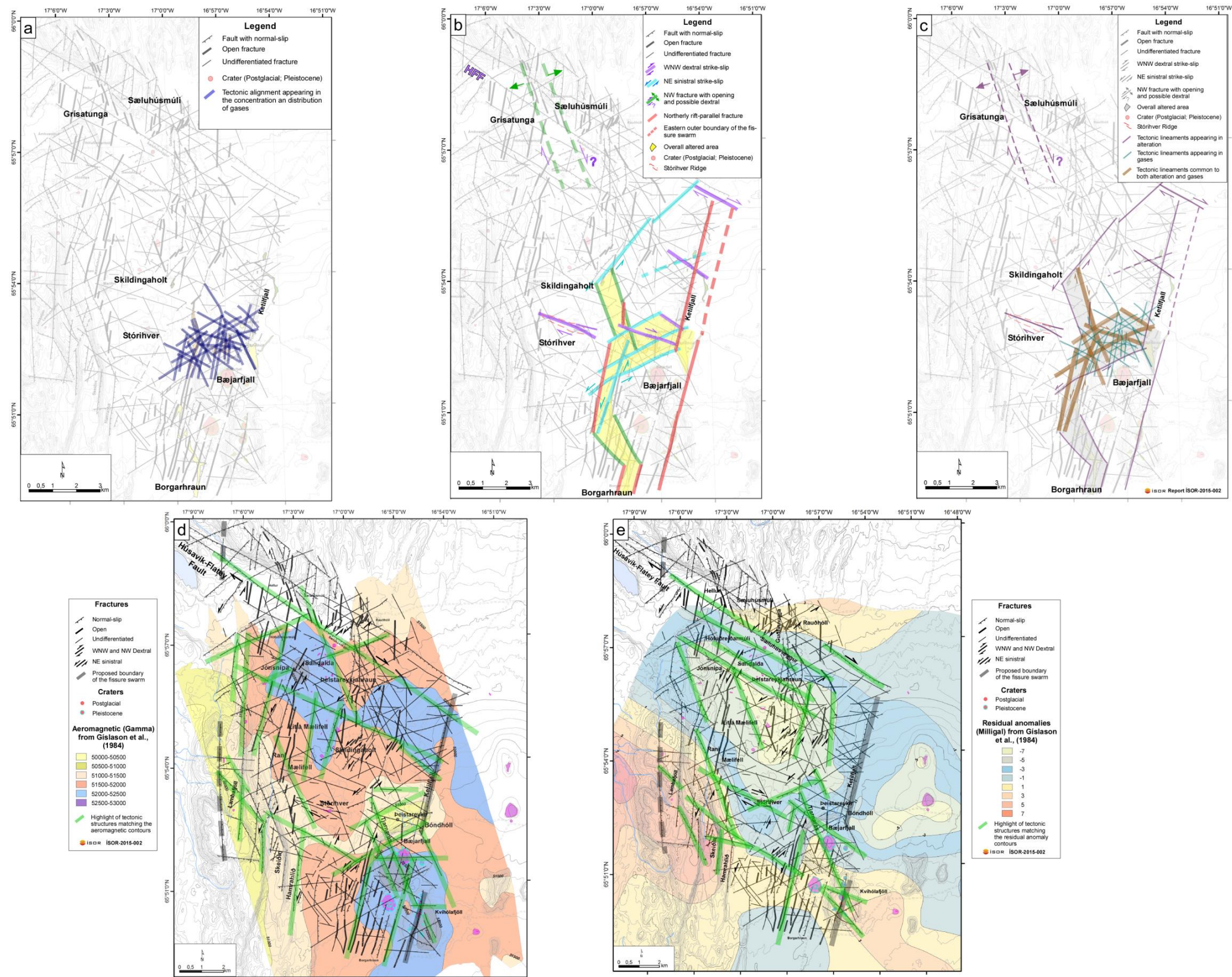


Figure 4. Recall of some results from Phases 1 and 2 (3): (a), (b) and (c) Respectively, correlation of the structural pattern with tectonic lineations emerging from the distribution of gases, the alteration block, and the structures common to alteration and gases distribution. (d) and (e) Respectively, correlation of the structural pattern with the aeromagnetic and Bouguer gravity anomaly maps obtained by Gíslason et al. (1984).

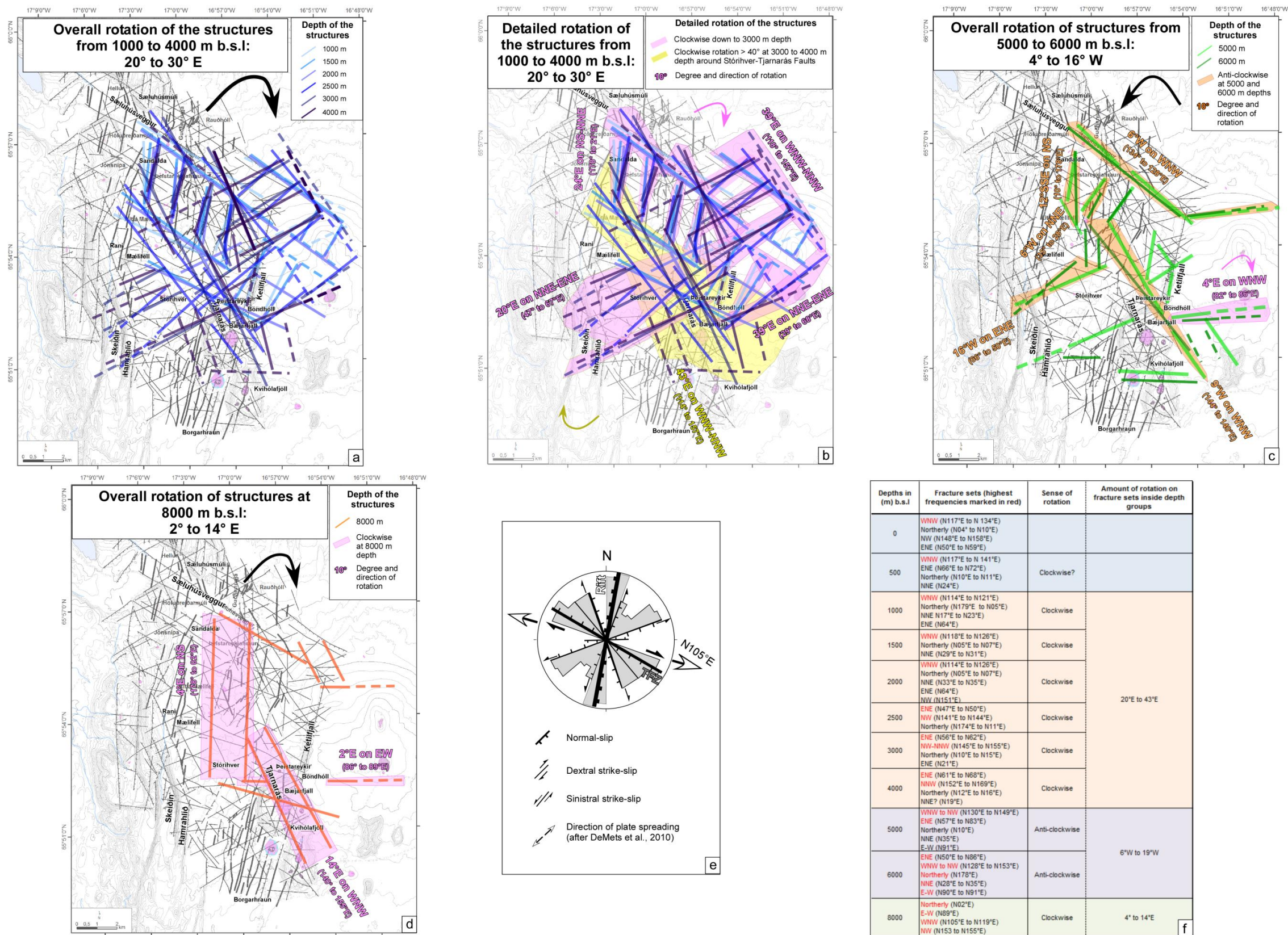


Figure 5. Recall of some results from Phases 1 and 2 (4): Correlation of the structural pattern with the lineations emerging from the resistivity anomalies at: (a) and (b) 1000 to 4000 m b.s.l. (c) 5000 m to 6000 m, and 8000 m b.s.l., including the clockwise and anticlockwise rotations. (e) Structural sets controlling the resistivity anomalies indicative of rift and transform mechanisms. (f) Depths at which individual fracture sets are most dominant.

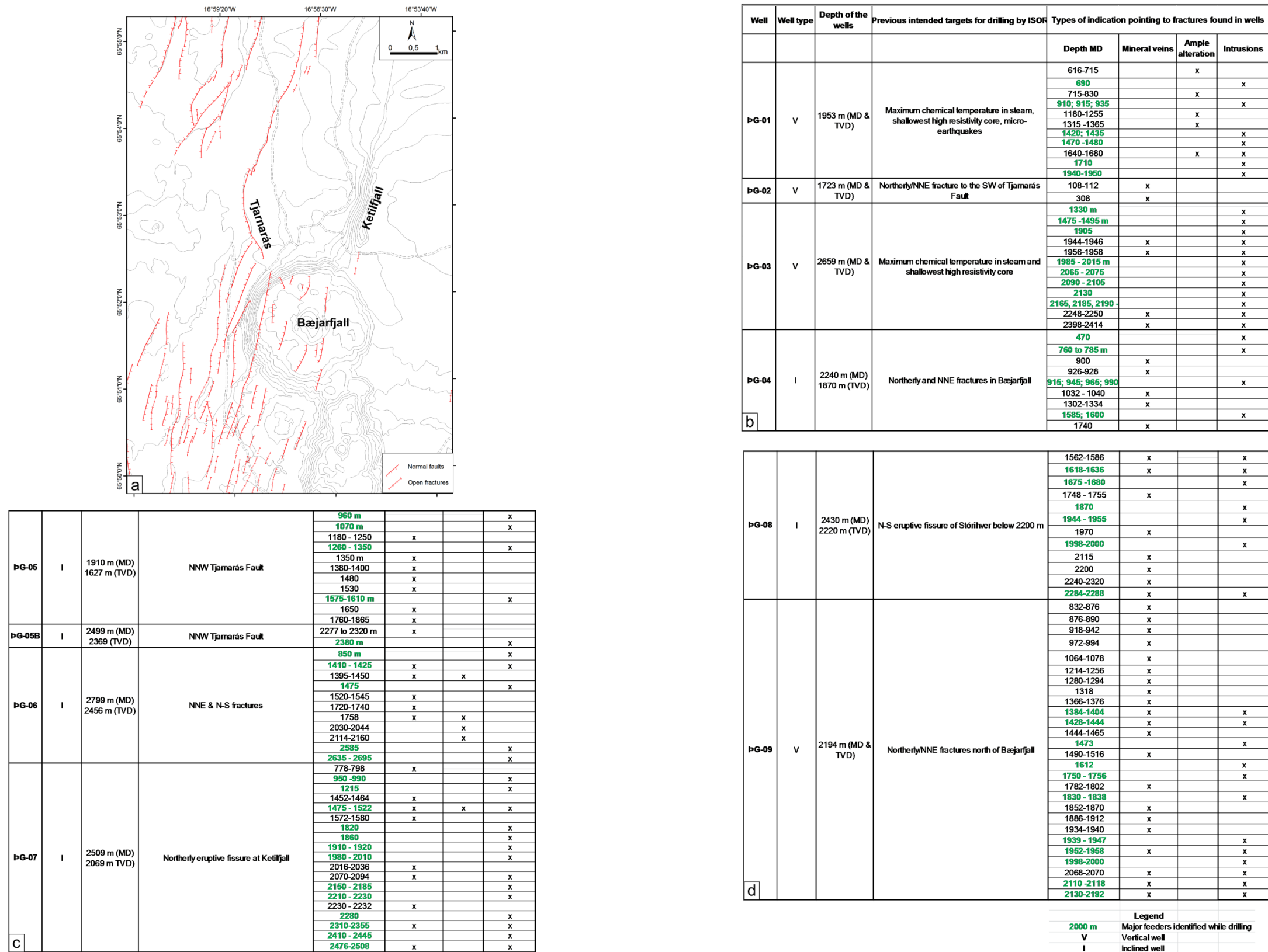


Figure 6. Previous structural targets intended by drilling and findings in Deistareykir wells. (a) Northerly fractures used as drilling targets at Deistareykir. (b) to (d) Various indications of fracturing and their depth-intervals indicating more fractures (and sets) present at depth in each of the nine drilled wells.

Well	Well type	Depth of the wells (TVD above sea level or from boreplatform)	Intersected fractures as suggested from this study (Figures 7 and 8)			Summary of intersected permeable fractures and feeders from this study	Depth of feeders (m) MD	Depth of feeders (m) TVD	Feeders in wells projected at the surface in terms of horizontal distance from well head	Mwe (Production capacity of the well)	
			Horizontal distance of fractures to the feeder, projected on well path and presented as distance from well head	Strike of fractures	Dip of fractures	Fault numbers for figures 9 and 10					
ÞG-01	V	1953 m (MD & TVD)	~ 110 m from feeder	FAULT 1: N 67° E	If fault dips 80-85° SE (same fault as in ÞG-05?)	F13	1620 m to 1640 m	1620 m to 1640 m	0 m	7.3	
ÞG-05	I	1910 m (MD) 1627 m (TVD)	~ 210 m	FAULT 1: N 67° E	If fault dips ~ 80-85° SE (same fault as ÞG-01?)	F13	890 m	840 m	170	0	
			~ 350 m	FAULT 2: N 49° E	If fault dips 86° NW	F10	1380 m to 1400 m	1275 m to 1295 m	440 to 460m		
ÞG-05B	I	2499 m (MD) 2369 (TVD)	~ 230 m	FAULT 1: N 67° E	If fault dips 80°-85° SE (same fault as in ÞG-01; ÞG-05)	F13	863 m	831	149 m	10.2	
			~ 200 m	FAULT 3: N165° E	If fault dips ~ 80-83° SW	F12	1535 m	1445 m	365 m		
			~ 440 m	FAULT 4: N158° E (Tjarnarás Fault)	Fault dips 85°-87° WSW	F11	2270 m	2165 m	~ 520m		
ÞG-02	V	1723 m (MD & TVD)	~ 30 m	FAULT 5: N 156° E	If fault dips 85° WSW	F9	657 m, 960 m, 1062 m	657 m, 960 m, 1062 m	0 m	0	
			~ 50 m	and/or FAULT 6: N 55° E	If fault dips ~ 85° NW	F7	657 m, 960 m, 1062 m	657 m, 960 m, 1062 m			
			~ 80 m	and/or FAULT 7: N 53° E	If fault dips ~ 85° SE	F6	960 m, 1062 m	960 m, 1062 m			
			~ 15 m	and/or FAULT 8: N 00° E	If fault dips ~ 85° W	F8	657 m, 960 m, 1062 m	657 m, 960 m, 1062 m			
ÞG-04	I	2240 m (MD) 1870 m (TVD)	~ 420 m	FAULT 9: N 08° E	If fault dips ~ 80° E	F14	1600	1390 m	600	20.9	
			~ 680 m	FAULT 10: N 54° E	If fault dips 85° SE	F15	1840	1603 m	770 m		
			~ 680 m	and/or FAULT 11: N 132° E	If fault dips 85° SW	F16	1840	1603 m			
ÞG-07	I	2509 m (MD) 2069 m (TVD)	Sub-parallel to ÞG-07 at the surface; ~ 70 m of feeder	FAULT 1: N 50° E	If fault dips ~ 85° NW	F25	750 m	721 m	135 m	4.1	
			~ 290 m	and/or FAULT 2: N116° E	If fault dips ~ 85° SW	F26	750 m	721 m			
			~ 890 m	Dyke of Ketilfjall: N 15°-20° E	If dyke dips ~ 82° E	DYKE 29	2325 m to 2345 m	1955 m to 1970 m			1105 to 1115m
			~ 1190 m	and/or FAULT 3: N101° E	If fault segments dip ~ 85° SW and NE	F28	2325 m to 2345 m	1955 m to 1970 m			
ÞG-03	V	2659 m (MD & TVD)	~ 50 m	FAULT 4: N 20° E	If fault dips 85°-87° W	F27	1610 m to 1680 m, 1880 m	1610 m to 1680 m, 1880 m	0 m	6.7	
			~ 50 m	and/or FAULT 1: N 50° E	If fault dips 85°-87° NW (same as in ÞG-07?)	F25	1610 m to 1680 m, 1880 m	1610 m to 1680 m, 1880 m			
ÞG-06	I	2799 m (MD) 2456 m (TVD)	~ 220 m	FAULT 5: N 54° E	If fault dips 85° SE	F23	846 m	811 m	165 m	6.7	
			~ 420 m	FAULT 6: N 40° E	If fault dips 85° SE	F22	1145 m	1098 m	315 m		
			~ 580 m	FAULT 7: N 57° E	If fault dips 85° NW	F21a	1720 m to 1740 m	1578 m to 1595 m	605 to 615m		
			~ 720 m	and/or FAULT 8: N 04° E	If fault dips 85° E	F19	1720 m to 1740 m	1578 m to 1595 m			
			~ 930 m	FAULT 9: N 06° E	If fault dips 85° W	F18	2674 m	2380 m	1150m		
~ 880 m	and/or FAULT 10: N 54° E	If fault dips 82° NW	F17	2674 m	2380 m						
ÞG-09	V	2194 m (MD & TVD)	~ 80 m	FAULT 11: N 02° E	If fault dips 85° W and is segmented at depth	F20	860 m, 1460 m, 2100 m	860 m, 1460 m, 2100 m	0 m	3.5	
			~ 90 m	and/or FAULT 7: N57° E	If fault segment dips 80°-85° SE (same fault as in ÞG-06)	F21b	1460 m, 2100 m	860 m, 1460 m, 2100 m			
			~ 70 m	and/or FAULT 12: N117° E	If fault dips 80°-85° SW	F24	860 m, 1460 m, 2100 m	860 m, 1460 m, 2100 m			
ÞG-08	I	2430 m (MD) 2220 m (TVD)	~ 550 - 850 m fault zone	FAULT 1 in ENE fault zone: 69° E	Fault zone dipping 80°-83° SE	F1	1680 m, 1748 m, 1773 m	1520 m, 1590 m, 1610 m	603, 640, 655m	0	
			~ 750 m	and/or FAULT 2: N 06° E to N 20° E	If fault dips 80°-83° E	F3	1680 m, 1748 m, 1773 m	1520 m, 1590 m, 1610 m			
			~ 550 - 850 m fault zone	FAULT 3 in ENE fault zone: N 67° E	Fault zone dipping 80°-83° SE	F2a; 2b	1680 m, 1748 m, 1773 m; 2260 m	1520 m, 1590 m, 1610 m, 2040 m			870m
			~ 900 m	and/or FAULT 4: N 11° E	If fault dips 80°-83° E	F4	2260 m	2040 m			
			~ 150 m of feeders	and/or FAULT 5: N111° E (Stöðhver dextral-oblique fault parallel to ÞG-08)	If fault dips 85° SW	F5	1680 m, 1748 m, 1773 m; 2260 m	1520 m, 1590 m, 1610 m, 2040 m			603, 640, 655m & 870 m

Figure 7. Basic parameters used for the structural analysis of fractures and feeders. The data about the wells and the depth of the feeders are from the borehole reports (ÍSOR database), but the values of production capacity are from Júlíusson (2015).

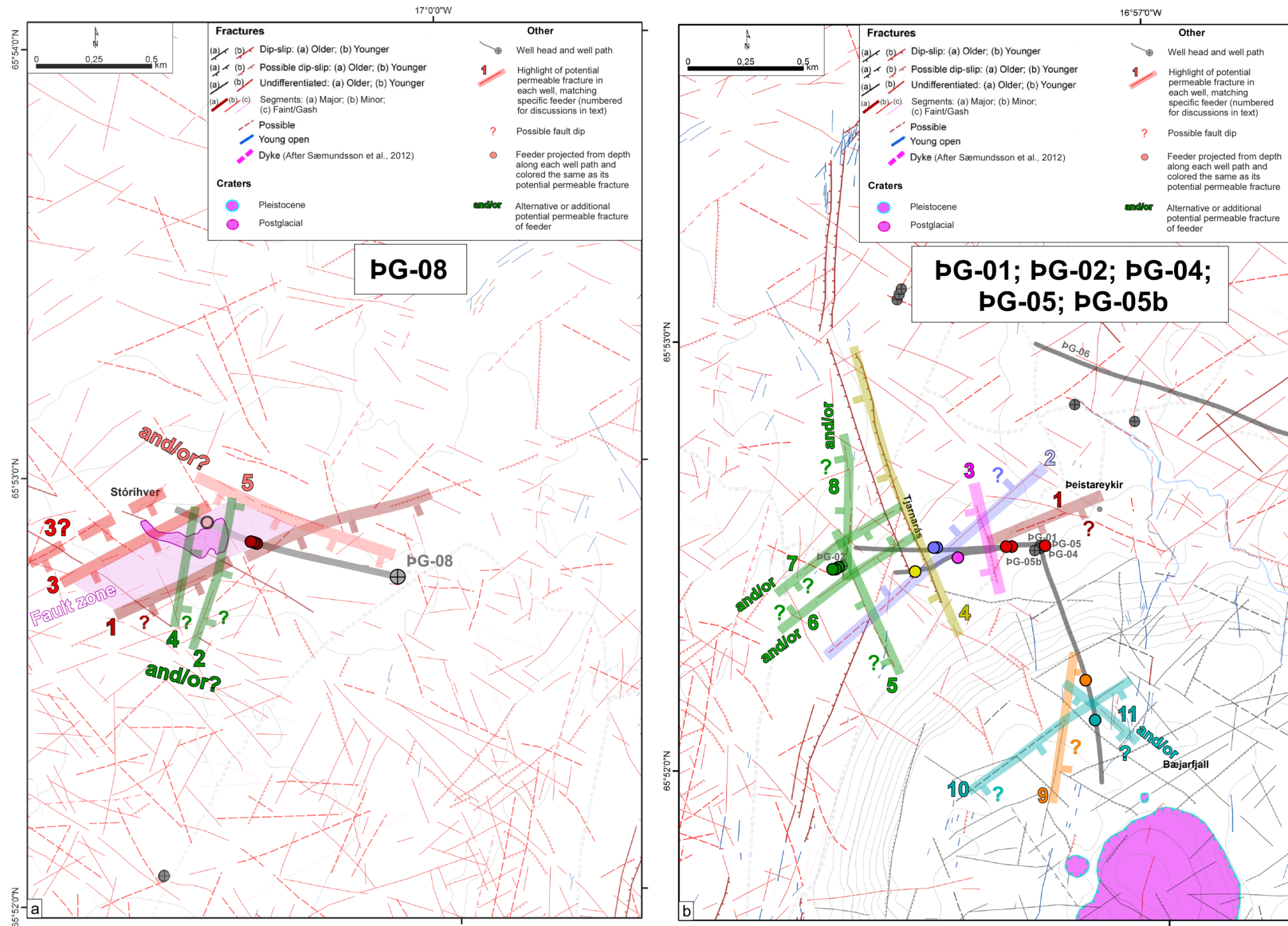


Figure 8. Feeders and potential permeable fractures (1). The feeders along each well along with corresponding permeable fractures. (a) The ENE, northerly and WNW sets and feeders in PG-8. (b) Dominantly NW and ENE, and secondarily northerly and WNW fractures controlling the feeders at the group of wells PG-1, PG-4, PG-5, and PG-5b. See Table 1 for background data used.

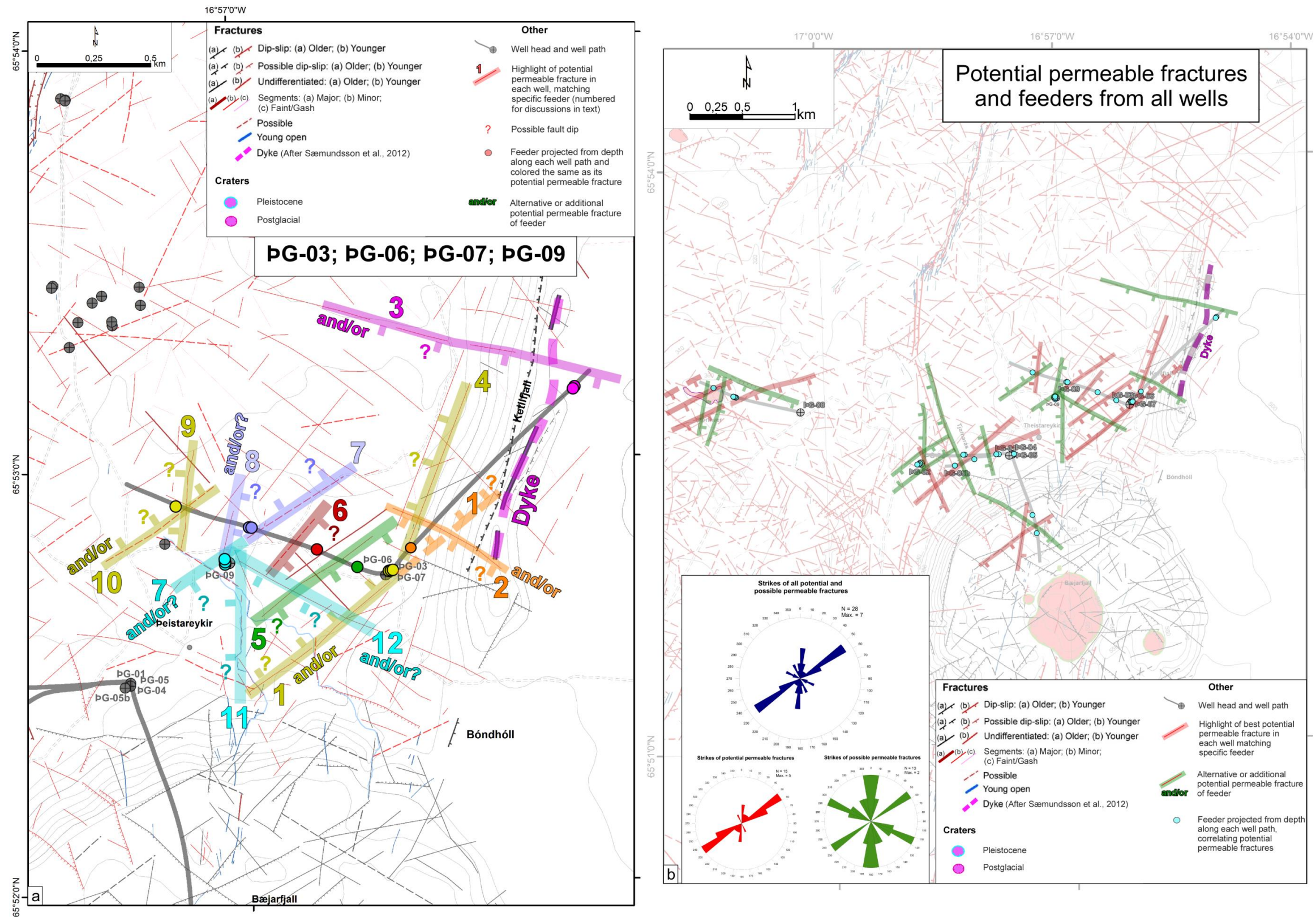
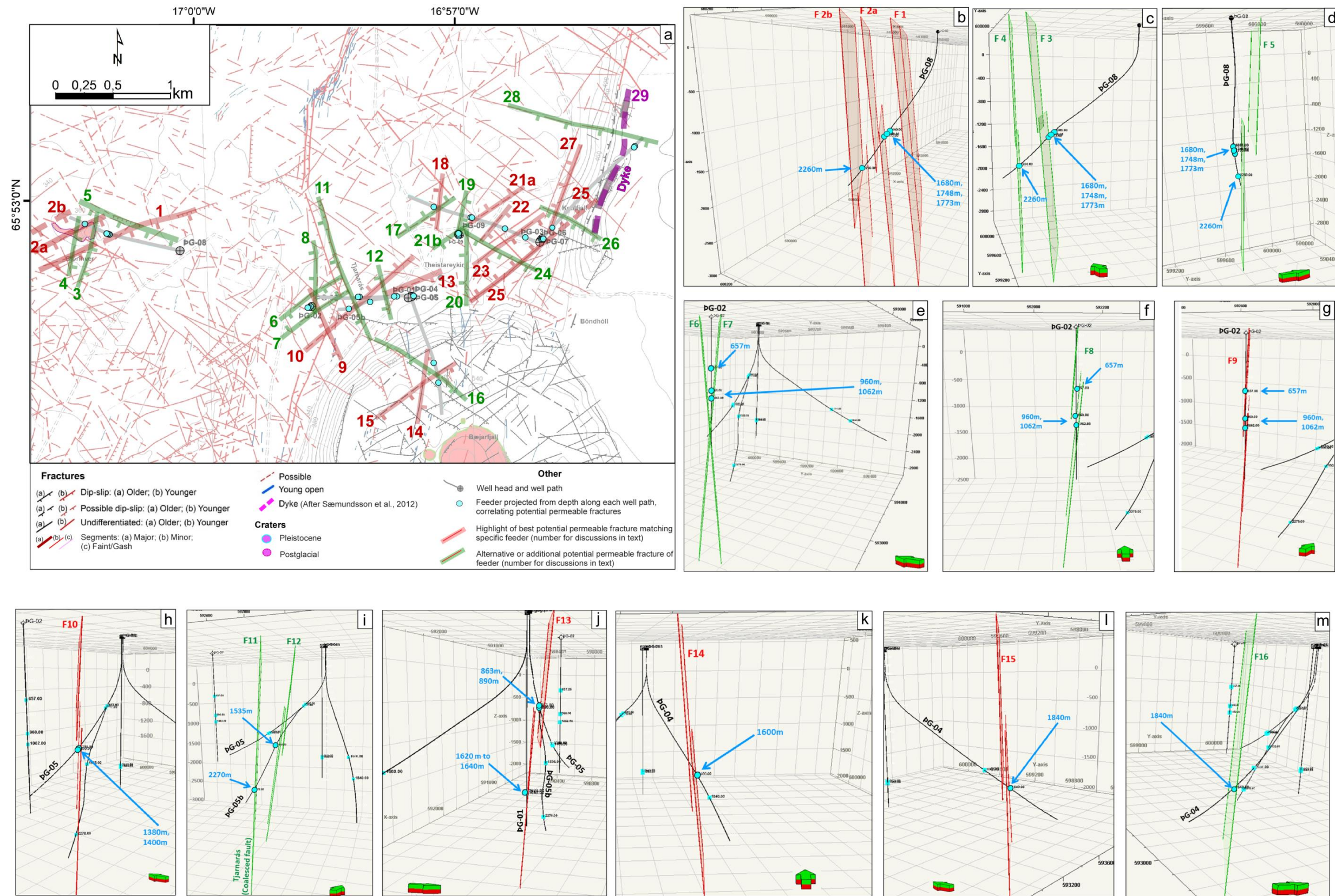
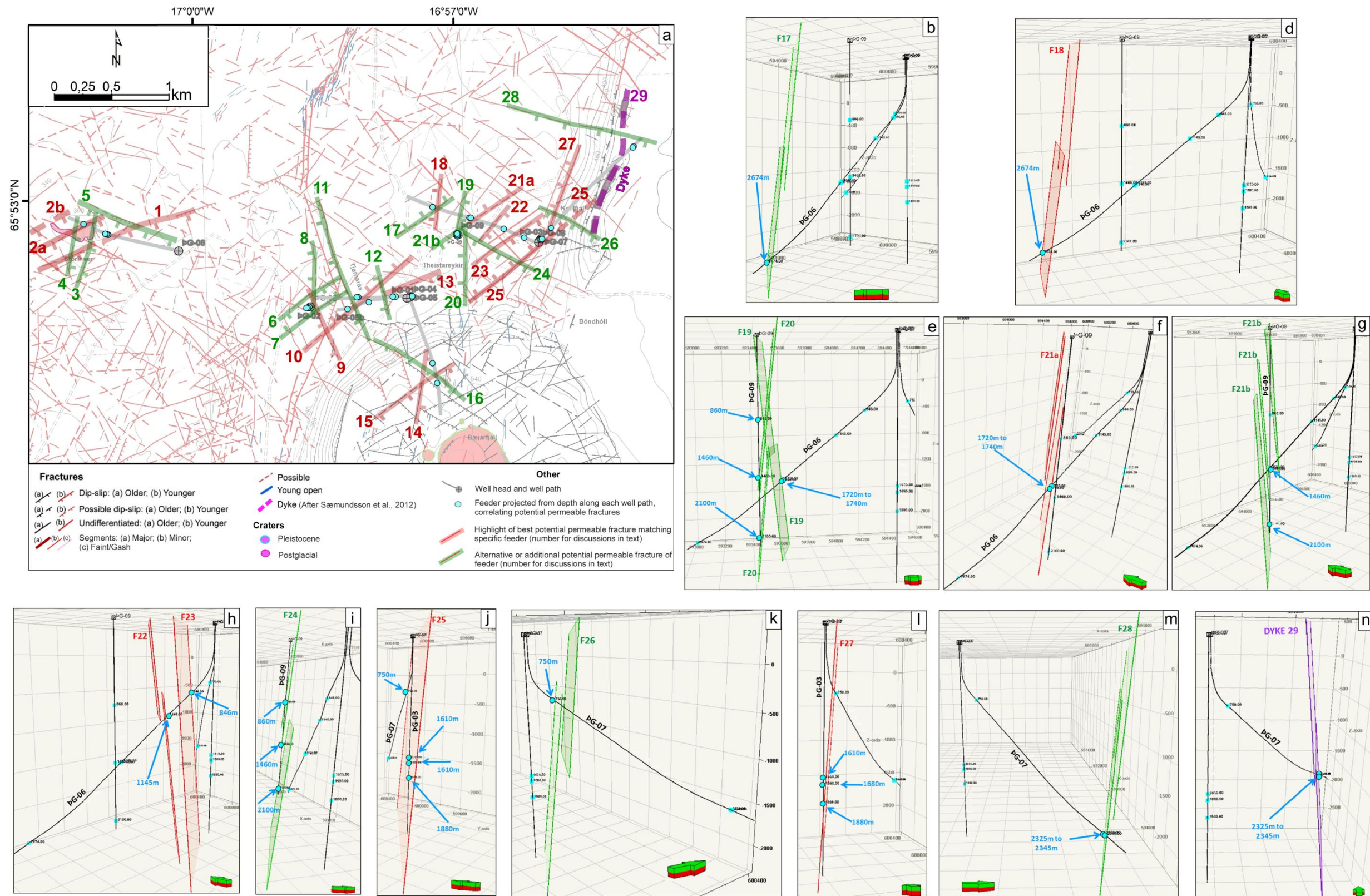


Figure 9. Feeders and potential permeable fractures (2). The feeders along each well along with corresponding permeable fractures. (a) The ENE, northerly and WNW sets and feeders in the group of wells pG-3, pG-6, pG-7, and pG-9. (b) Compilation of all permeable fractures and feeders on a single map, along with rose diagrams of all permeable fractures, potential permeable fractures and possible permeable structures. See Table 1 for background data used.





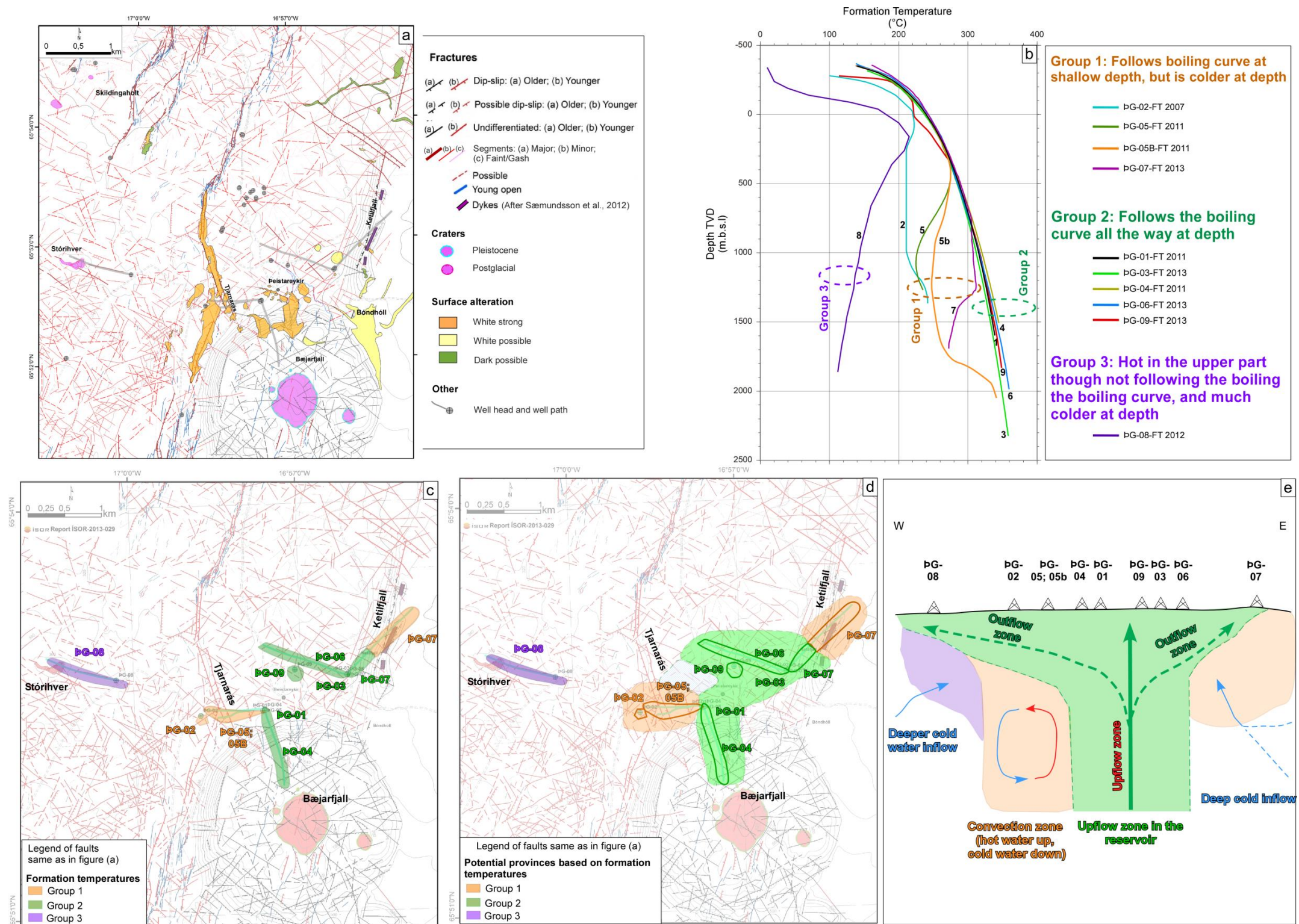


Figure 12. Provinces of formation temperatures. All depths are in TVD b.s.l. (a) Structural map and distribution of surface alteration as mapped from aerial images for reference (Khodayar and Björnsson, 2013). (b) Formation temperatures of the 10 drilled wells at Beistareykir and their classification in terms of groups. (c) The three groups in formation temperatures identified with colours along well paths. (d) Speculation as to the possible extent of the formation temperature provinces. (e) Schematic cross-section showing the configuration of the three groups, with the up-flow zone in the central part and the out-flow zones towards bG-7 and bG-8, respectively to the East and West. A convection zone may exist under bG-2, while the deeper parts of bG-8 and bG-7 could correspond to deep cold water inflow.

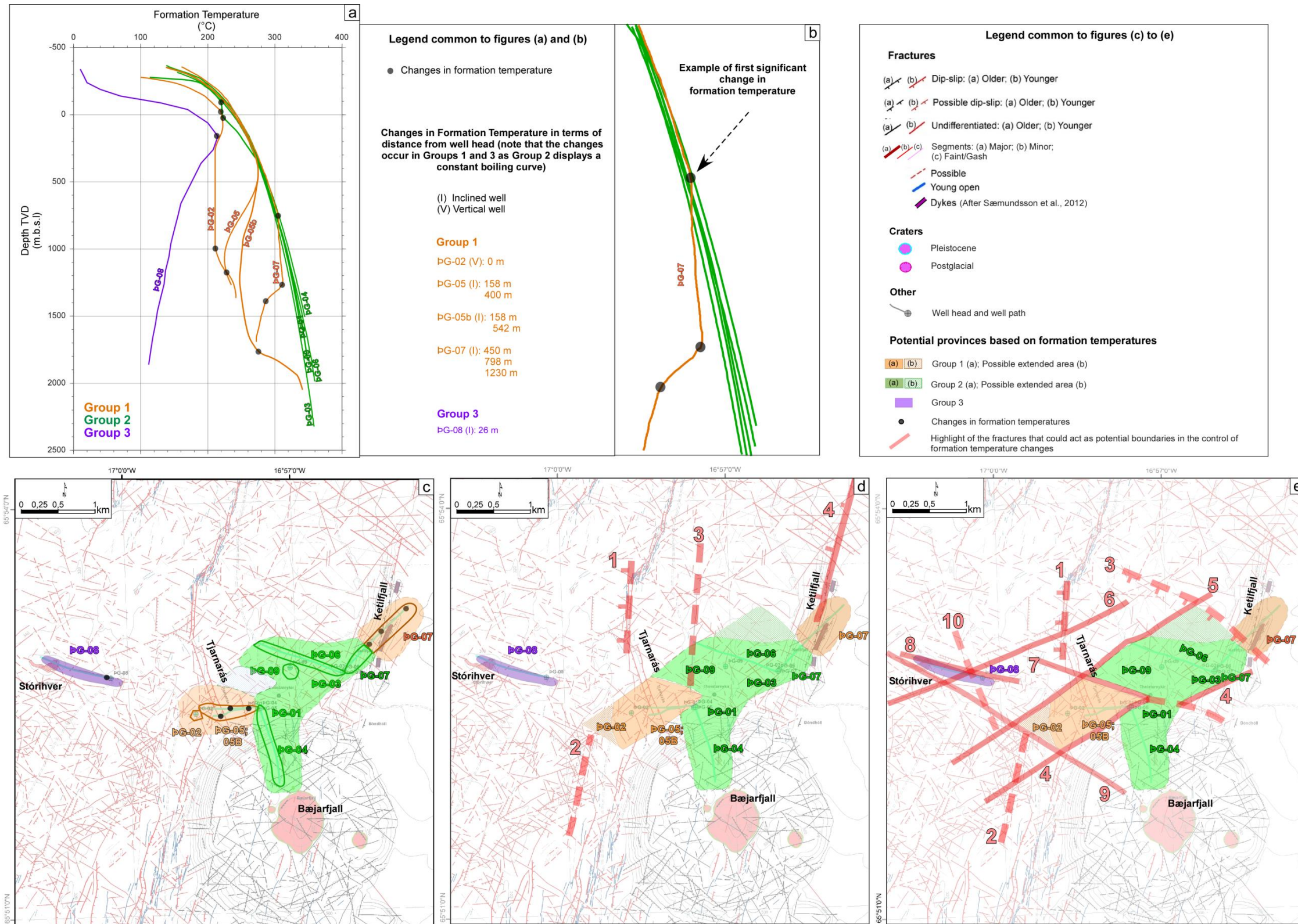


Figure 13. Changes in formation temperatures and potential structural control. (a) The wells coloured according to the three suggested groups in formation temperatures, and the points at which we interpreted the changes in temperatures. (b) Zoom on PG-7 showing how we interpreted the points of changes in the formation temperatures. (c) The formation temperature provinces and the points at which changes in the temperature occurred, as projected along well paths. (d) A first interpretation of the potential structures coinciding with the first changes in the formation temperatures, here solely the northerly set. (e) A second interpretation of the structural control of formation temperatures, taking into account the fracture segments of the rift and the transform zones. Numbers are for discussions in the text.

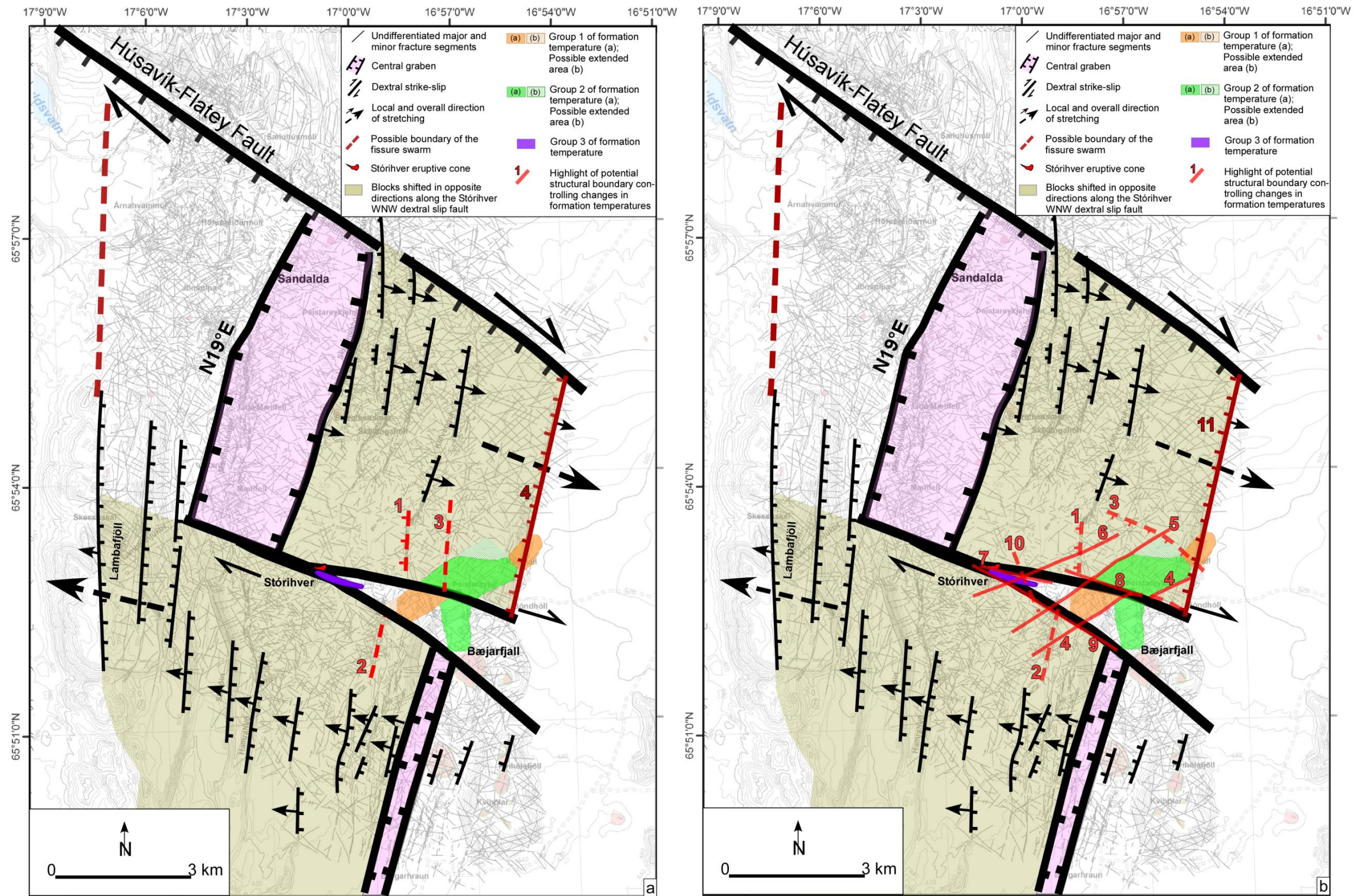


Figure 14. Structural interpretation of suggested fractures in formation temperatures in terms of the shift of Deistareykir fissure swarm on the WNW Stórihver-Bæjarfjall dextral Fault. (a) The suggested northerly segments seem not explaining as well the changes in the formation temperatures. Due to the shift of Deistareykir fissure swarm, the northerly structures to the north of Stórihver-Bæjarfjall Fault do not cross the WNW fault and thus are not explaining satisfactorily the compartmentalisation in the formation temperatures. (b) The combination of the Riedel shears and the northerly segments match best with the Stórihver-Bæjarfjall Fault itself, as well as with underlying fractures.

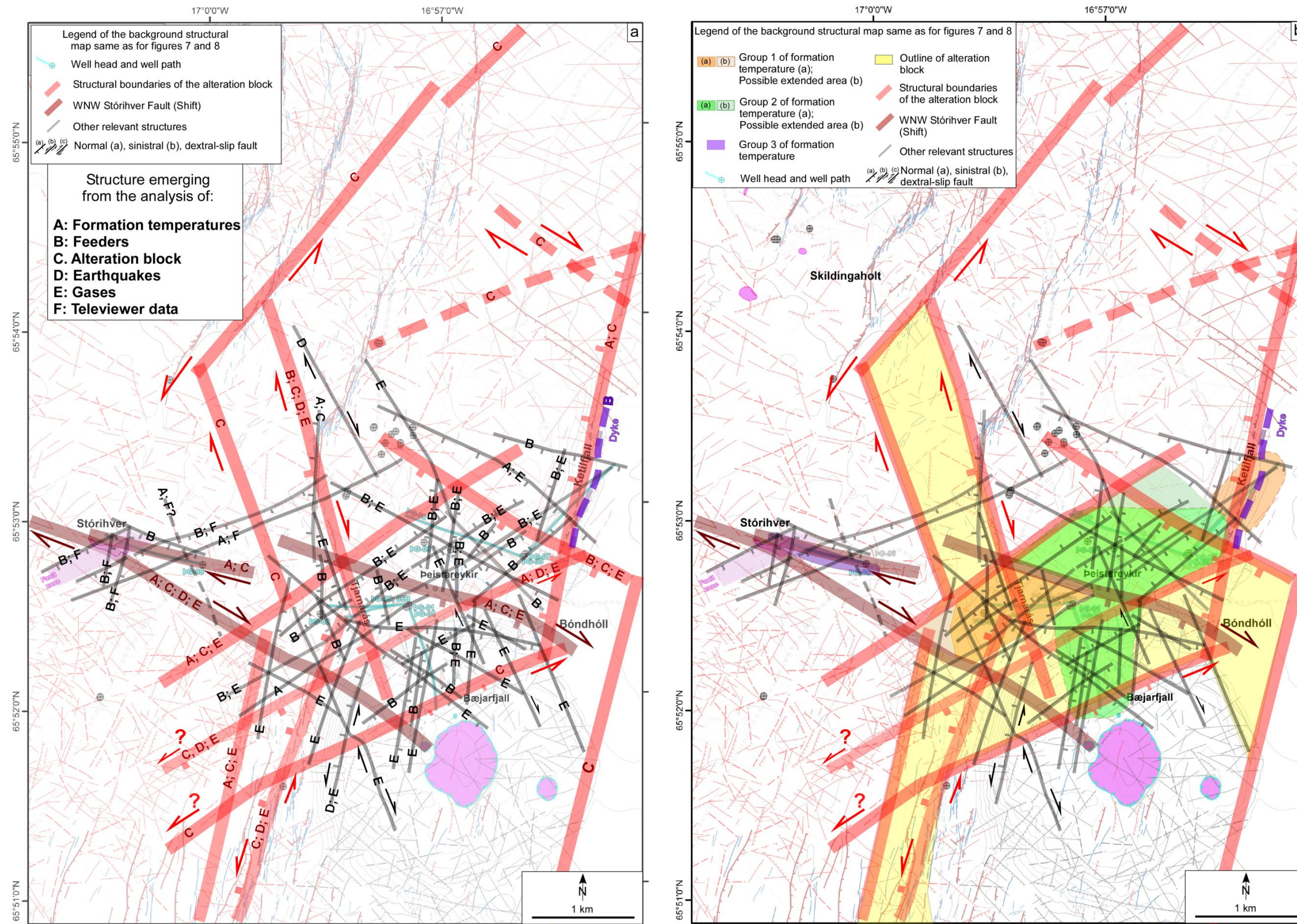


Figure 15. Compilation of the relevant multidisciplinary structural data, excluding the resistivity. (a) The main boundaries and comparatively the secondary fractures emerging in formation temperatures, feeders, surface alteration, earthquakes, gases, and televiever image logs. (b) The same structural pattern as in (a) superimposed on formation temperatures and the suspected configuration of surface alteration.

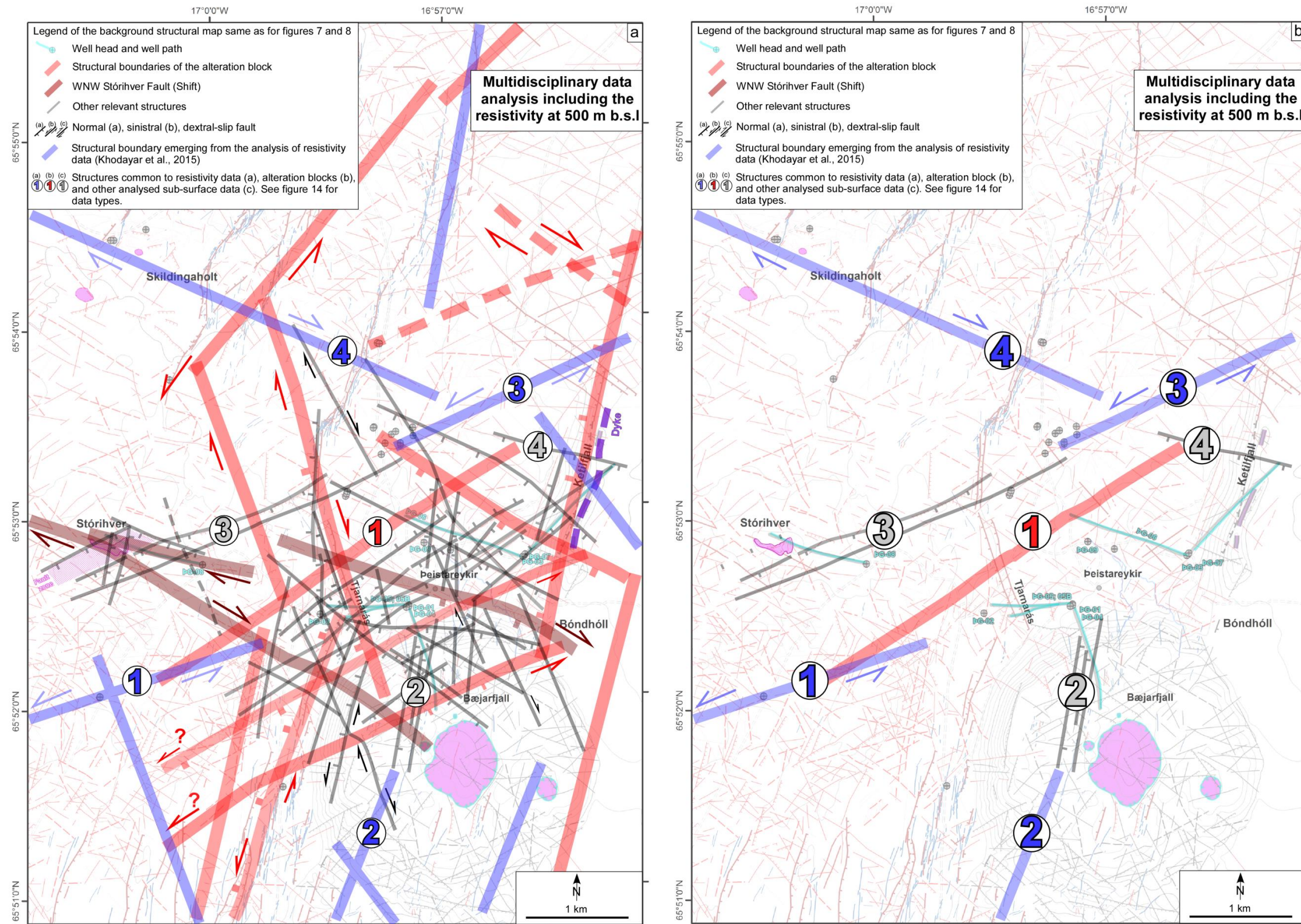


Figure 16. Compilation of the multidisciplinary structural data and lineations controlling the resistivity anomalies at 500 m b.s.l. (a) The lineations that seem controlling the resistivity anomalies are shown in blue, and superimposed on the multidisciplinary structural map where the common structures are shown with the same numbers. (b) Only the structures common to resistivity and the multidisciplinary structural map.

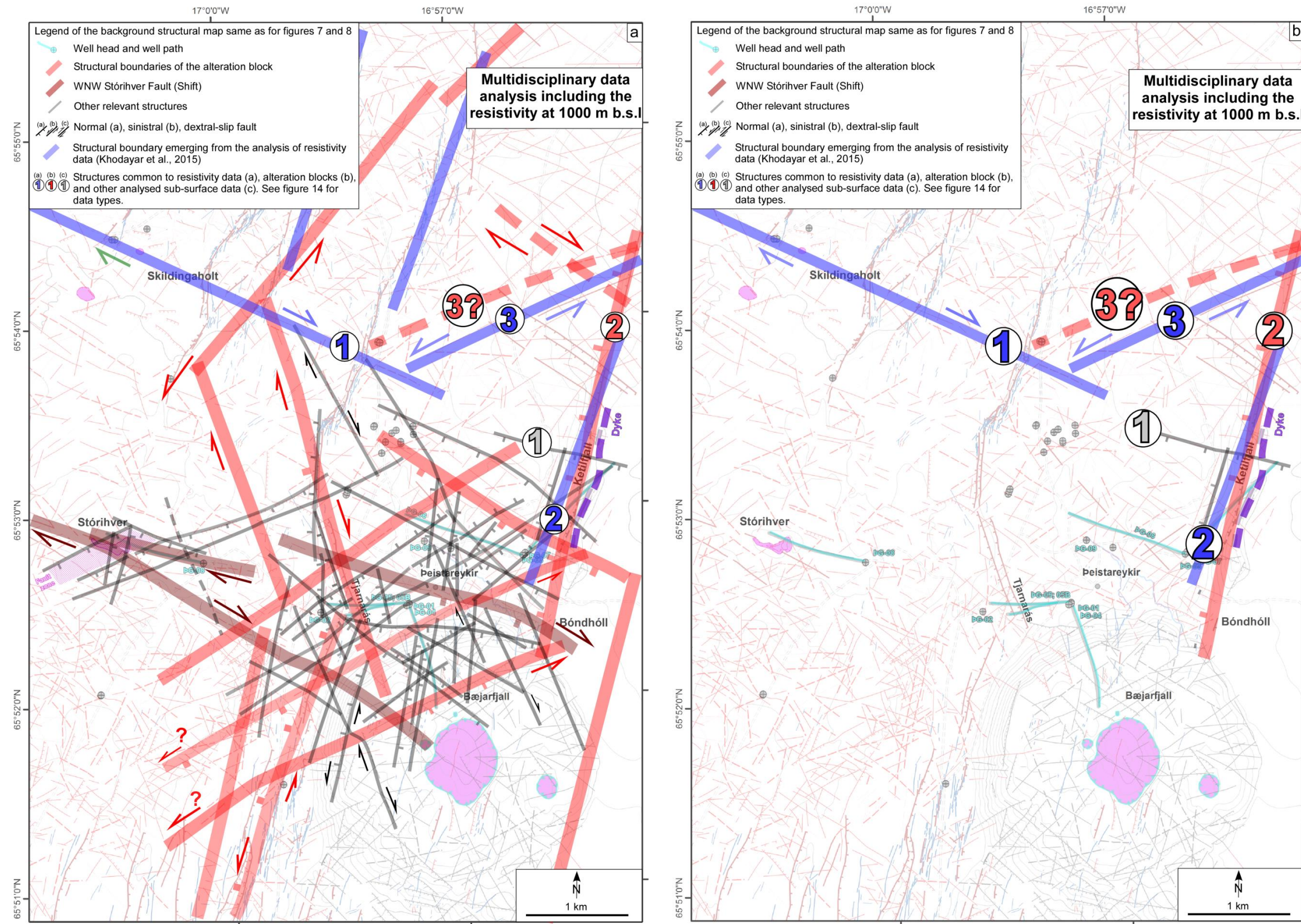


Figure 17. Compilation of the multidisciplinary structural data and lineations controlling the resistivity anomalies at 1000 m b.s.l. (a) The lineations that seem controlling the resistivity anomalies are shown in blue, and superimposed on the multidisciplinary structural map where the common structures are shown with the same numbers. (b) Only the structures common to resistivity and the multidisciplinary structural map.

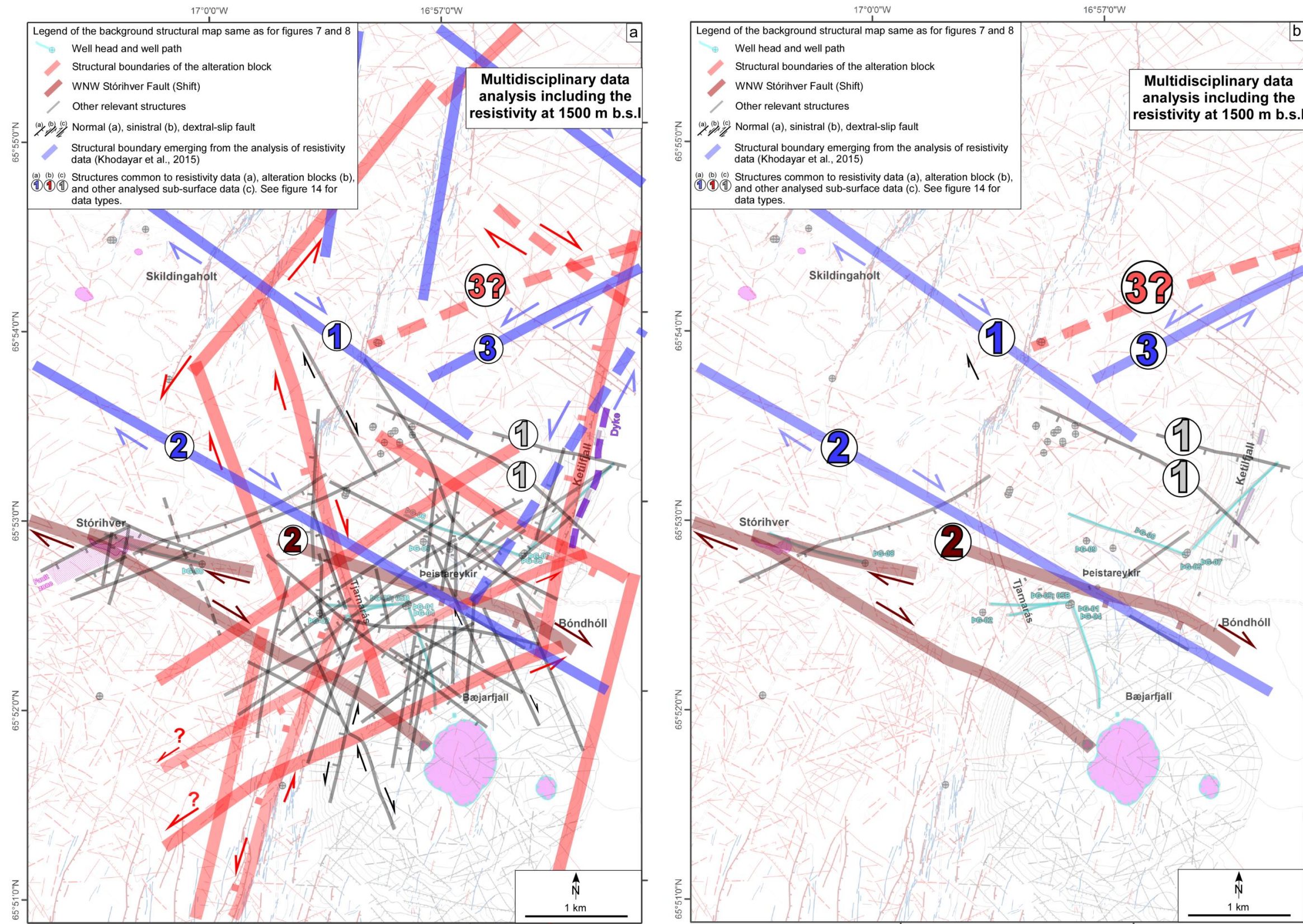


Figure 18. Compilation of the multidisciplinary structural data and lineations controlling the resistivity anomalies at 1500 m b.s.l. (a) The lineations that seem controlling the resistivity anomalies are shown in blue, and superimposed on the multidisciplinary structural map where the common structures are shown with the same numbers. (b) Only the structures common to resistivity and the multidisciplinary structural map.

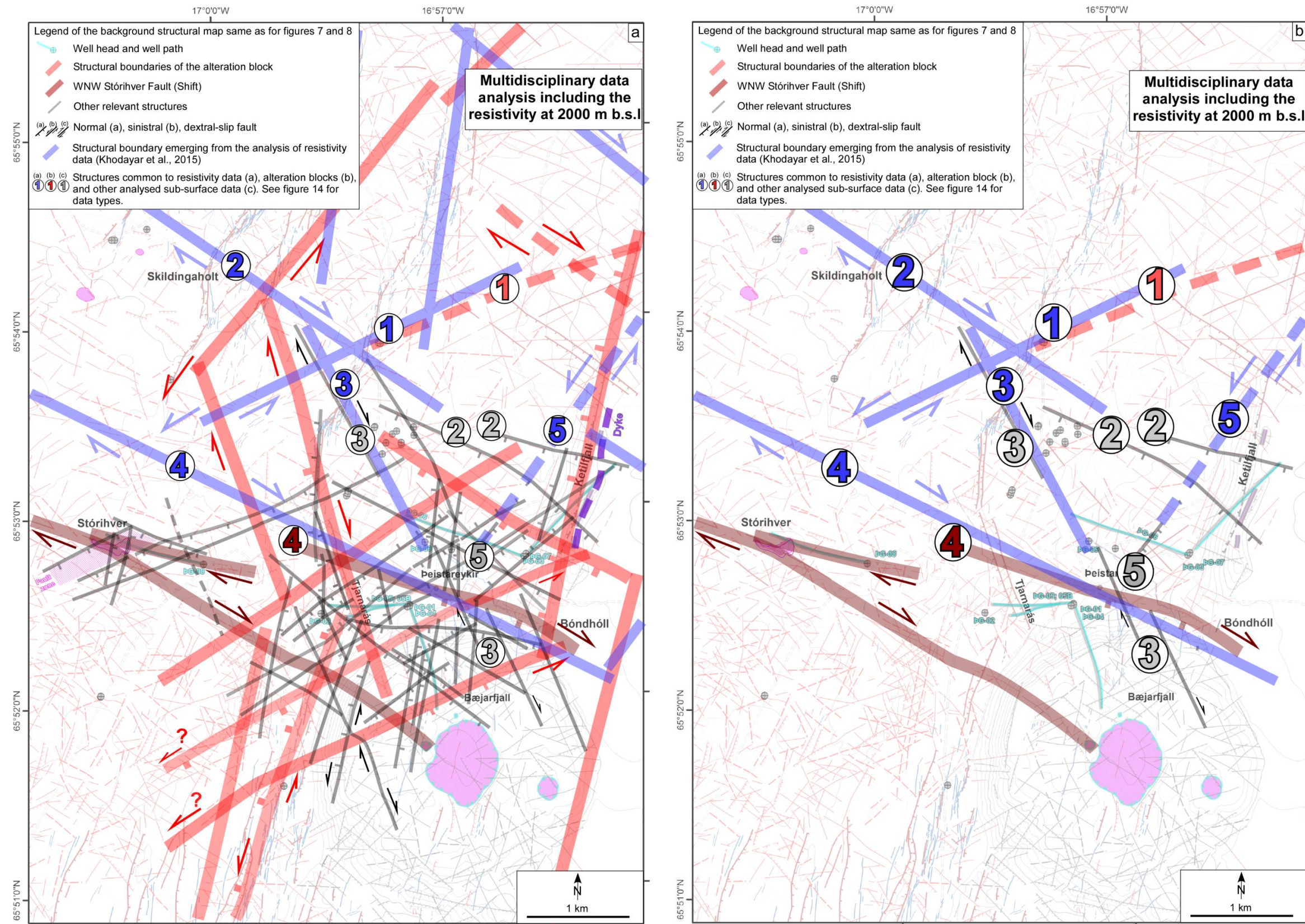


Figure 19. Compilation of the multidisciplinary structural data and lineations controlling the resistivity anomalies at 2000 m b.s.l. (a) The lineations that seem controlling the resistivity anomalies are shown in blue, and superimposed on the multidisciplinary structural map where the common structures are shown with the same numbers. (b) Only the structures common to resistivity and the multidisciplinary structural map.

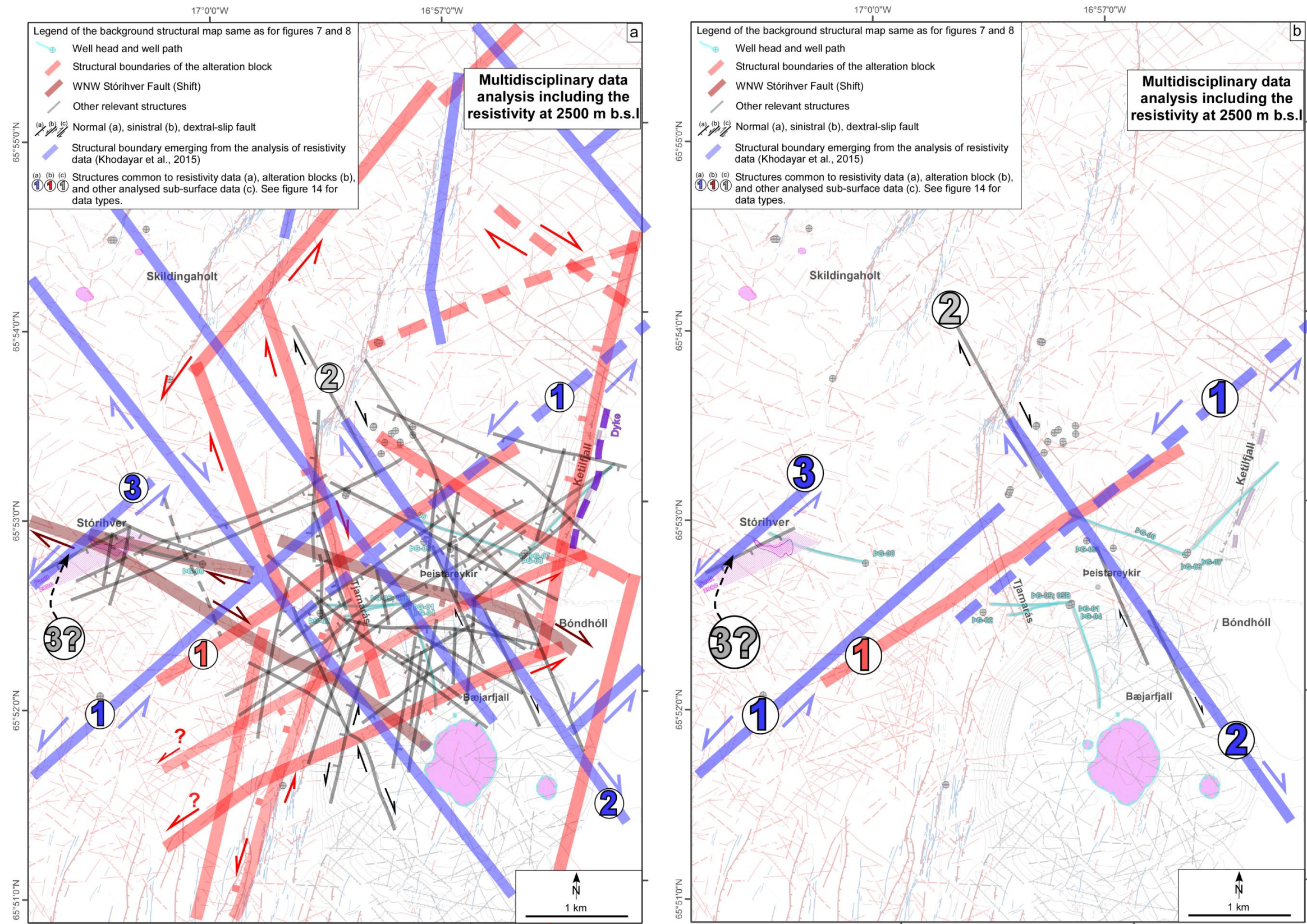


Figure 20. Compilation of the multidisciplinary structural data and lineations controlling the resistivity anomalies at 2500 m b.s.l. (a) The lineations that seem controlling the resistivity anomalies are shown in blue, and superimposed on the multidisciplinary structural map where the common structures are shown with the same numbers. (b) Only the structures common to resistivity and the multidisciplinary structural map.

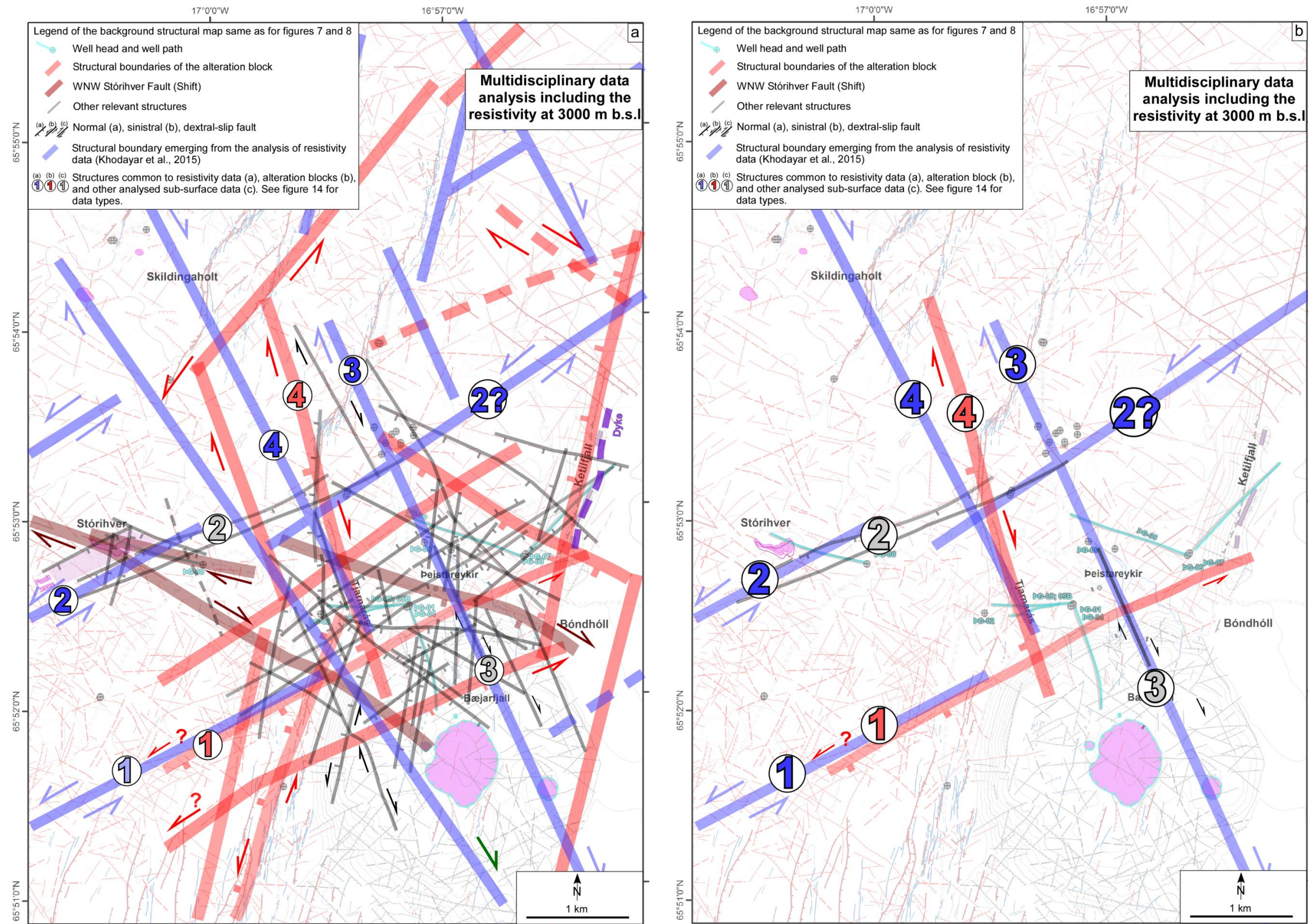


Figure 21. Compilation of the multidisciplinary structural data and lineations controlling the resistivity anomalies at 3000 m b.s.l. (a) The lineations that seem controlling the resistivity anomalies are shown in blue, and superimposed on the multidisciplinary structural map where the common structures are shown with the same numbers. (b) Only the structures common to resistivity and the multidisciplinary structural map.

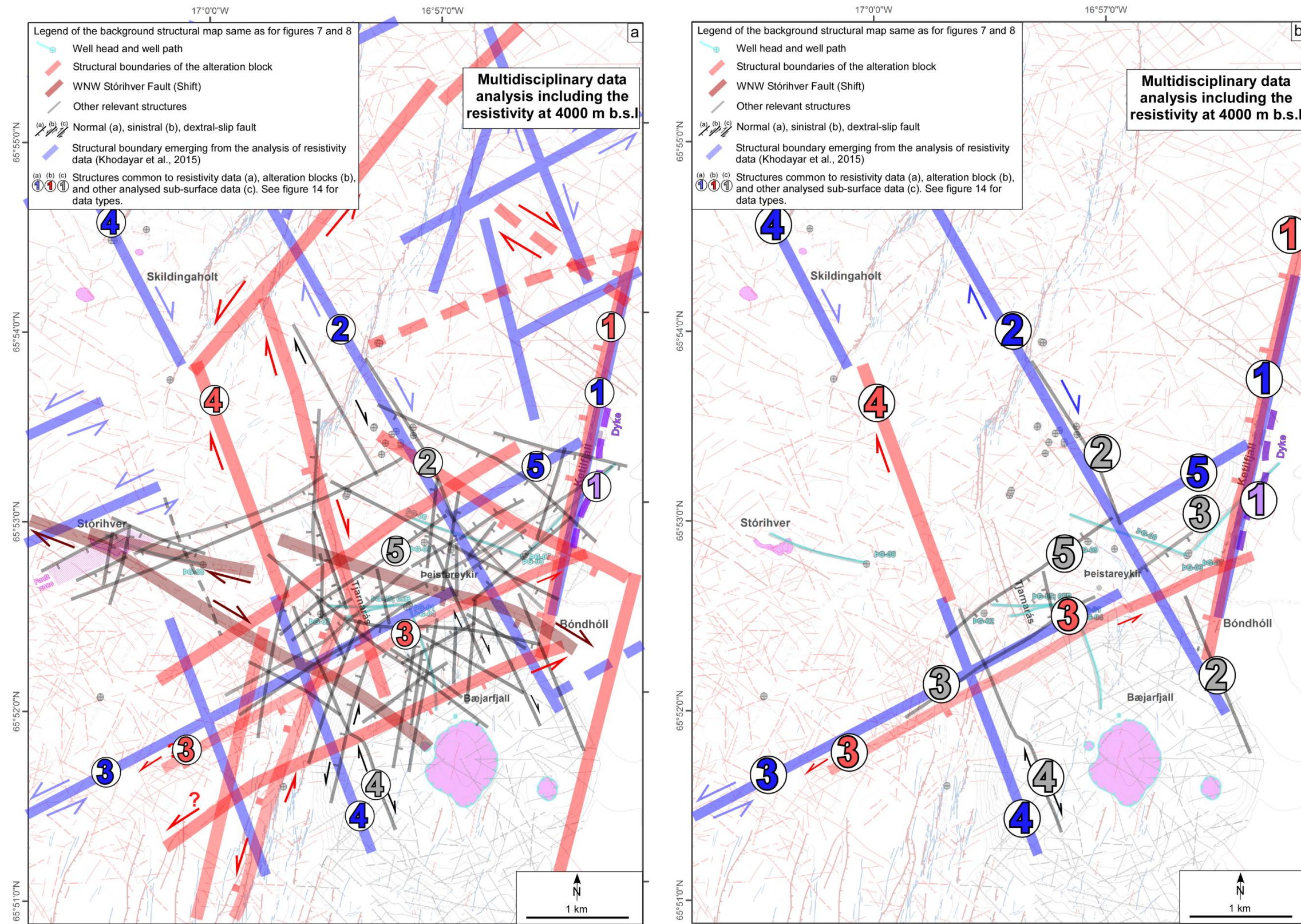


Figure 22. Compilation of the multidisciplinary structural data and lineations controlling the resistivity anomalies at 4000 m b.s.l. (a) The lineations that seem controlling the resistivity anomalies are shown in blue, and superimposed on the multidisciplinary structural map where the common structures are shown with the same numbers. (b) Only the structures common to resistivity and the multidisciplinary structural map.

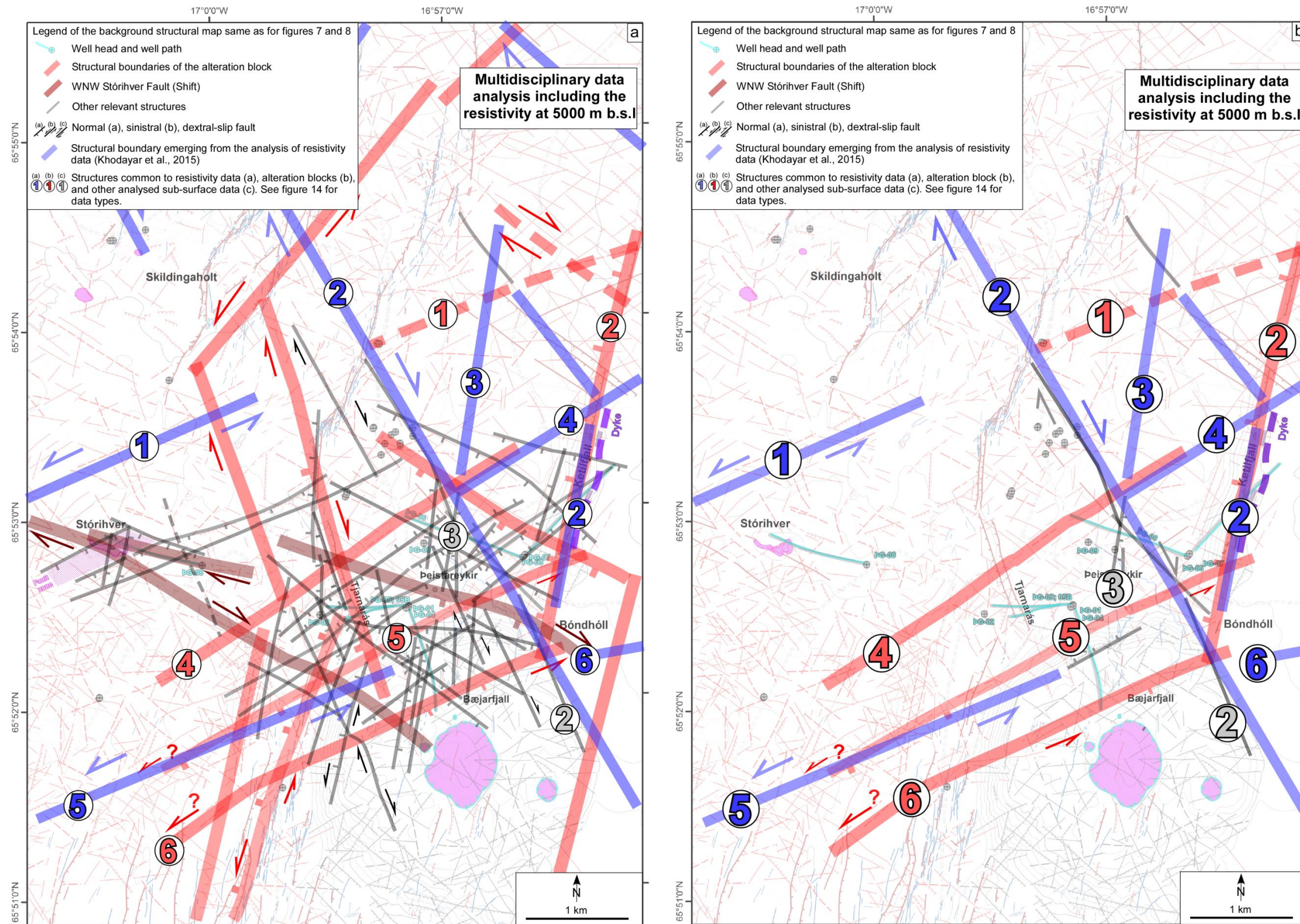


Figure 23. Compilation of the multidisciplinary structural data and lineations controlling the resistivity anomalies at 5000 m b.s.l. (a) The lineations that seem controlling the resistivity anomalies are shown in blue, and superimposed on the multidisciplinary structural map where the common structures are shown with the same numbers. (b) Only the structures common to resistivity and the multidisciplinary structural map.

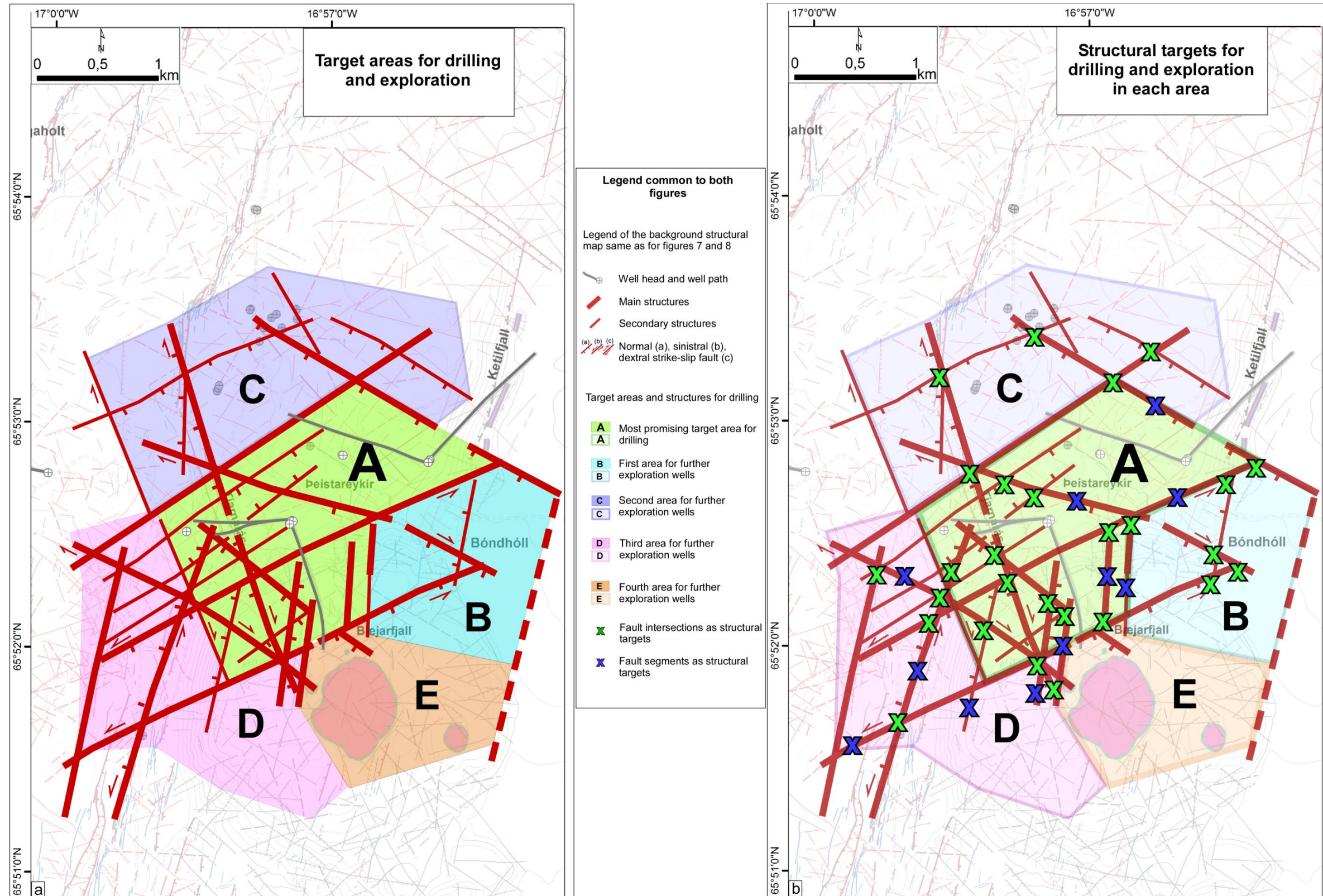
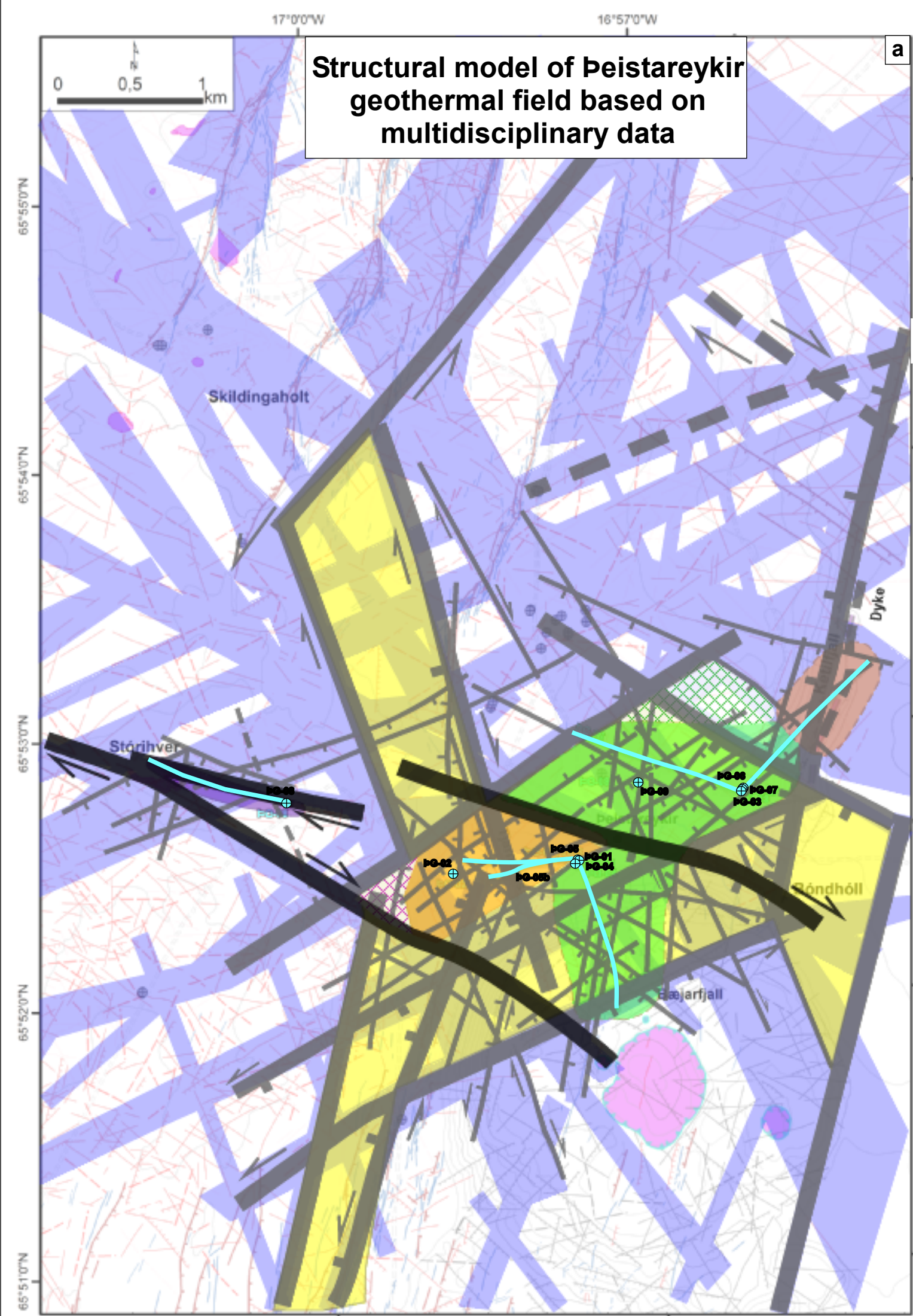


Figure 24. Suggested areas and structural targets for drilling. (a) The five suggested areas for drilling, where area (A) should provide Landsvirkjun with enough energy sought for the first stage of the power plant. Areas (B) to (D) are for further drilling exploration to provide additional information such as the size of the reservoir, the up-flow zone, and permeability at depth. (b) Structural targets belonging to rift and transform plate boundaries. The targets are mostly fracture intersections but also a few fracture traces.



Legend common to Map 1a to 1c

Faint background structural map

Fractures

- (a) (b) Dip-slip: (a) Older; (b) Younger
- (a) (b) Possible dip-slip: (a) Older; (b) Younger
- (a) (b) Undifferentiated: (a) Older; (b) Younger
- (a) (b) (c) Segments: (a) Major; (b) Minor; (c) Faint/Gash
- Possible
- Young open
- Dyke (After Sæmundsson et al., 2012a)

Craters

- Pleistocene
- Postglacial

Multidisciplinary data

Provinces in formation temperature (see text for definition)

- Group 1 of formation temperature (a); Possible extended area (b)
- Group 2 of formation temperature (a); Possible extended area (b)
- Group 3 of formation temperature

Surface alteration

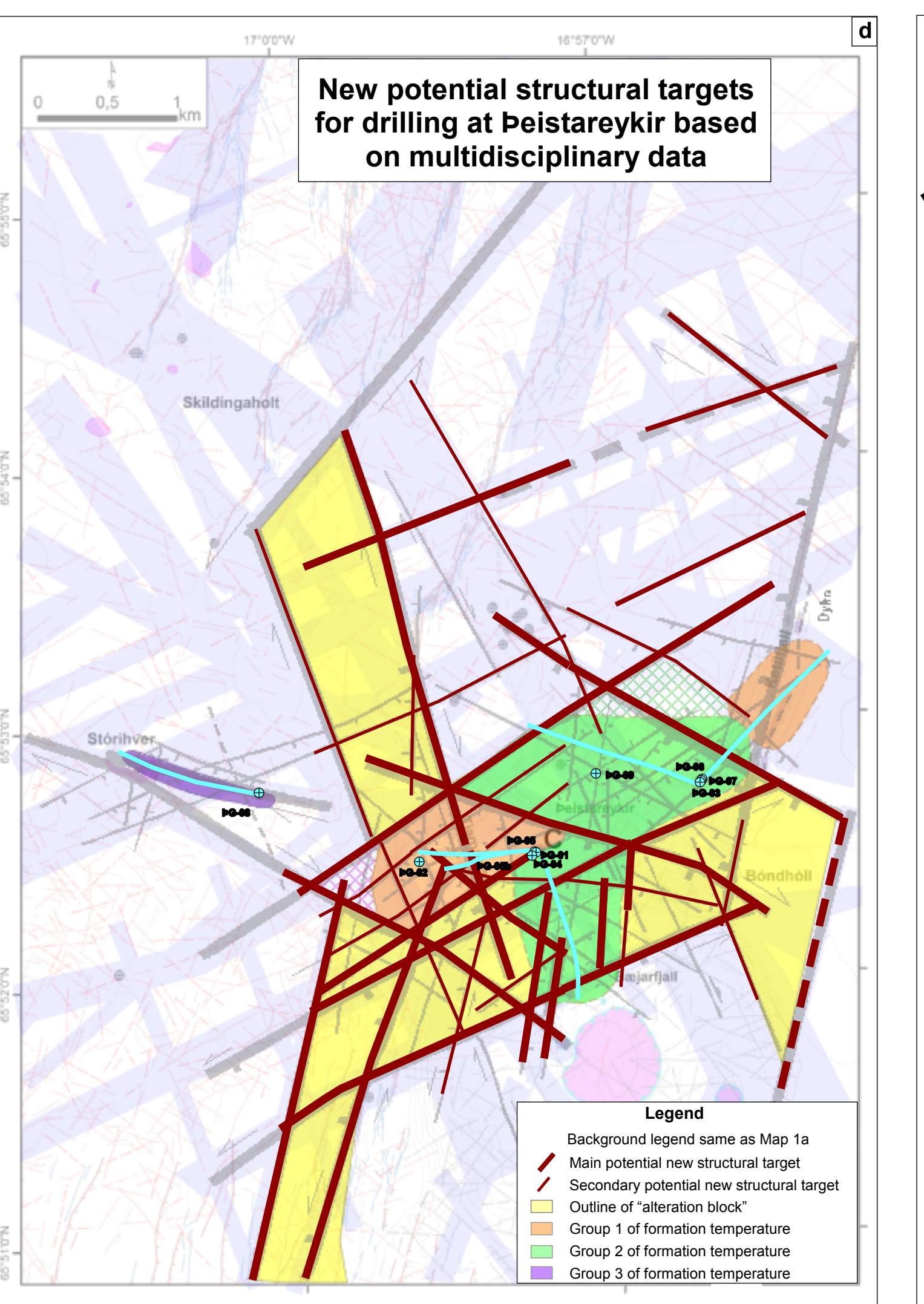
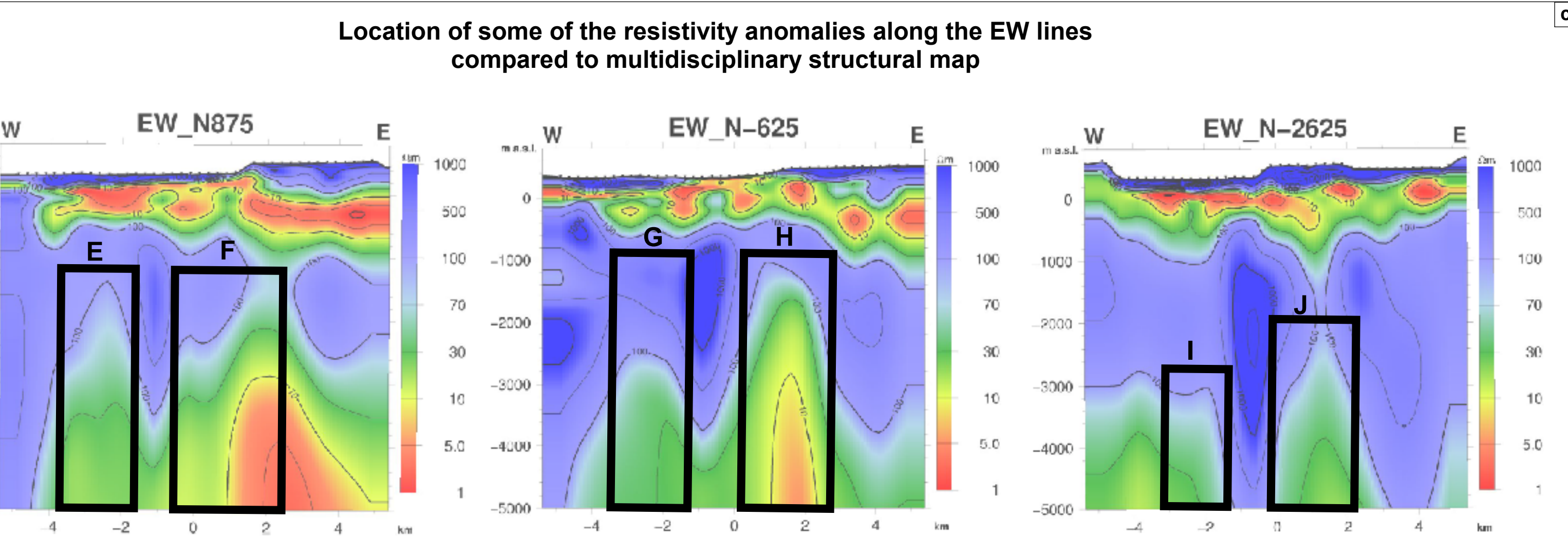
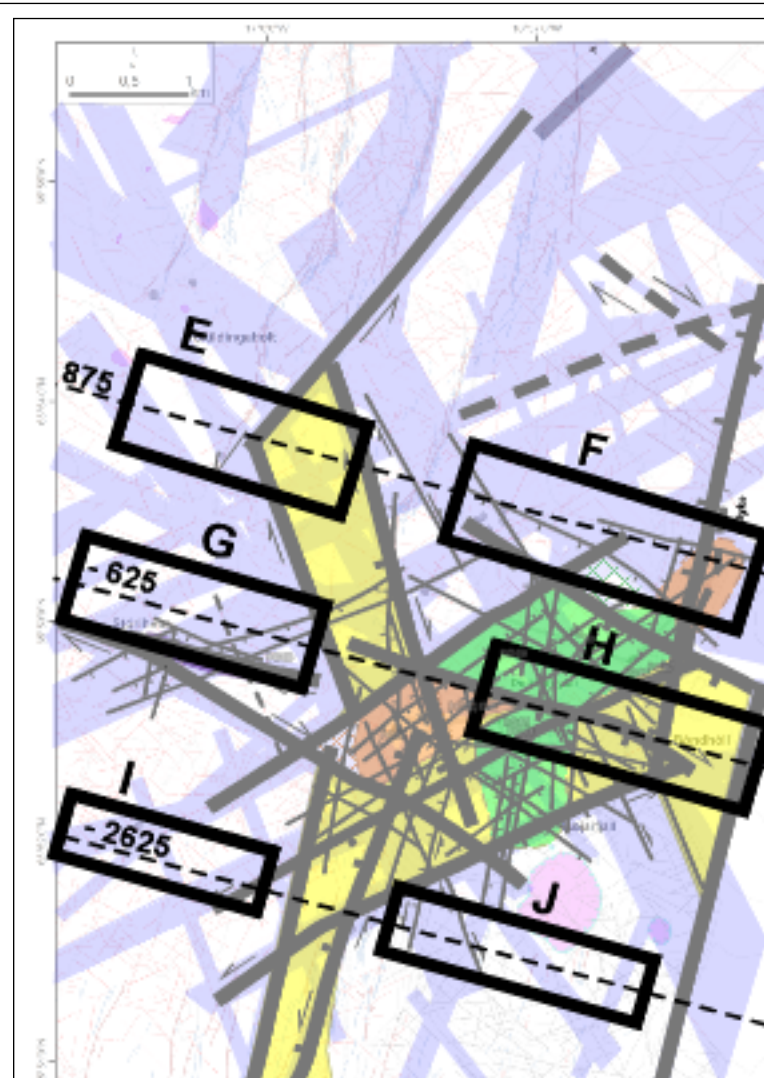
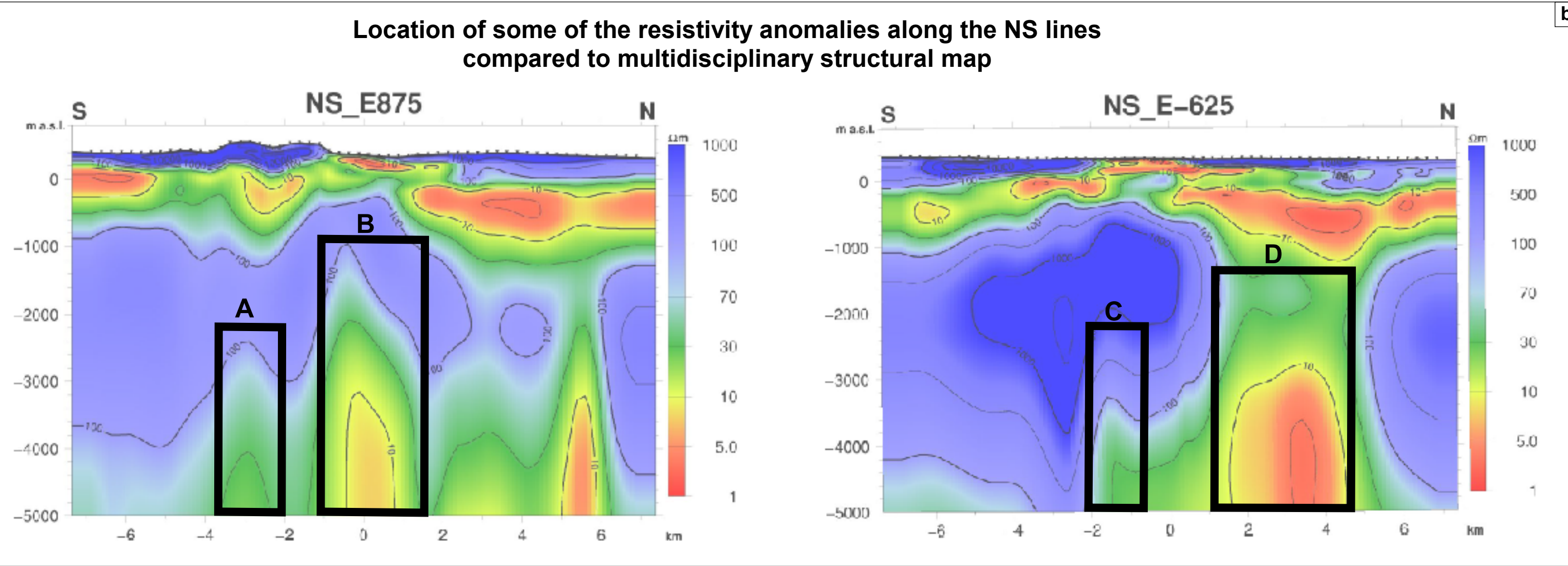
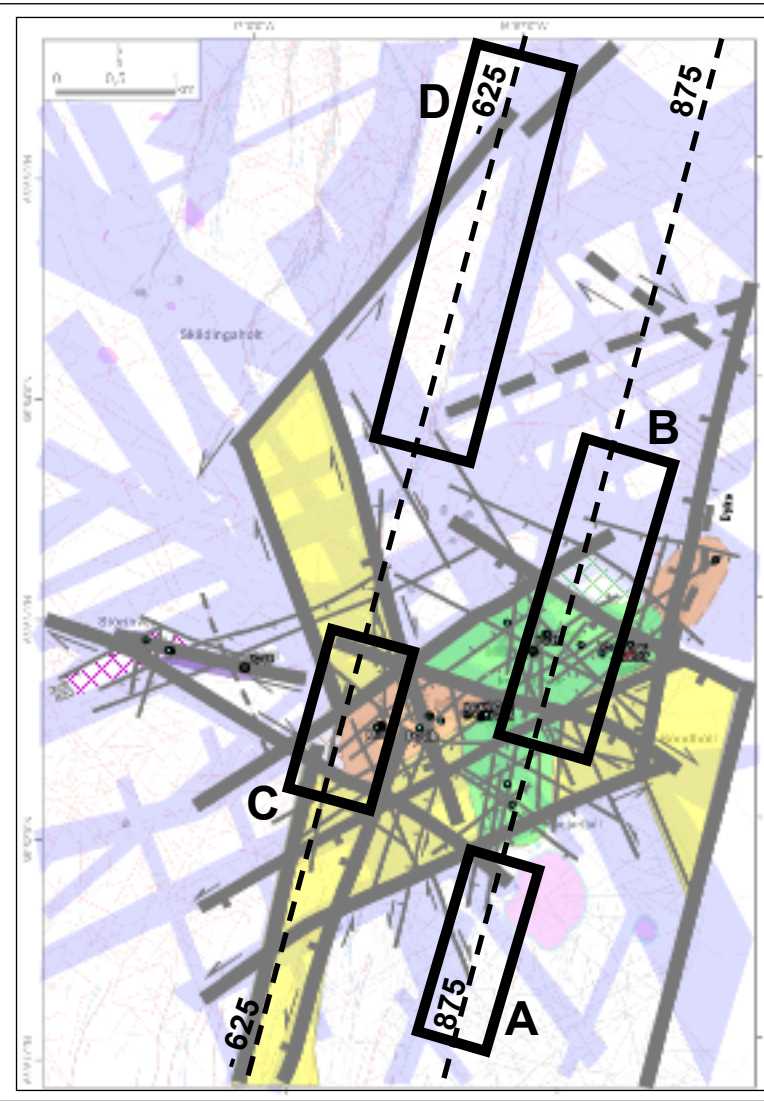
- Outline of alteration block containing all immediate surface alteration

Highlights of structures emerging from multidisciplinary data analysis and their motions

- Structural boundaries of the alteration block
- WNW Stórhver Fault (Shift)
- Other potential permeable fractures in each well matching specific feeder
- (a) (b) (c) Normal (a), sinistral (b), dextral-slip fault
- Structural boundary emerging from the analysis of resistivity data at various depths (Khodayar et al., 2015)

Resistivity anomalies along selected NS and EW lines (base data from Karlsdóttir et al., 2012)

- Highlight of same relevant resistivity anomaly on both cross-section and map
- Location of selected resistivity lines on map

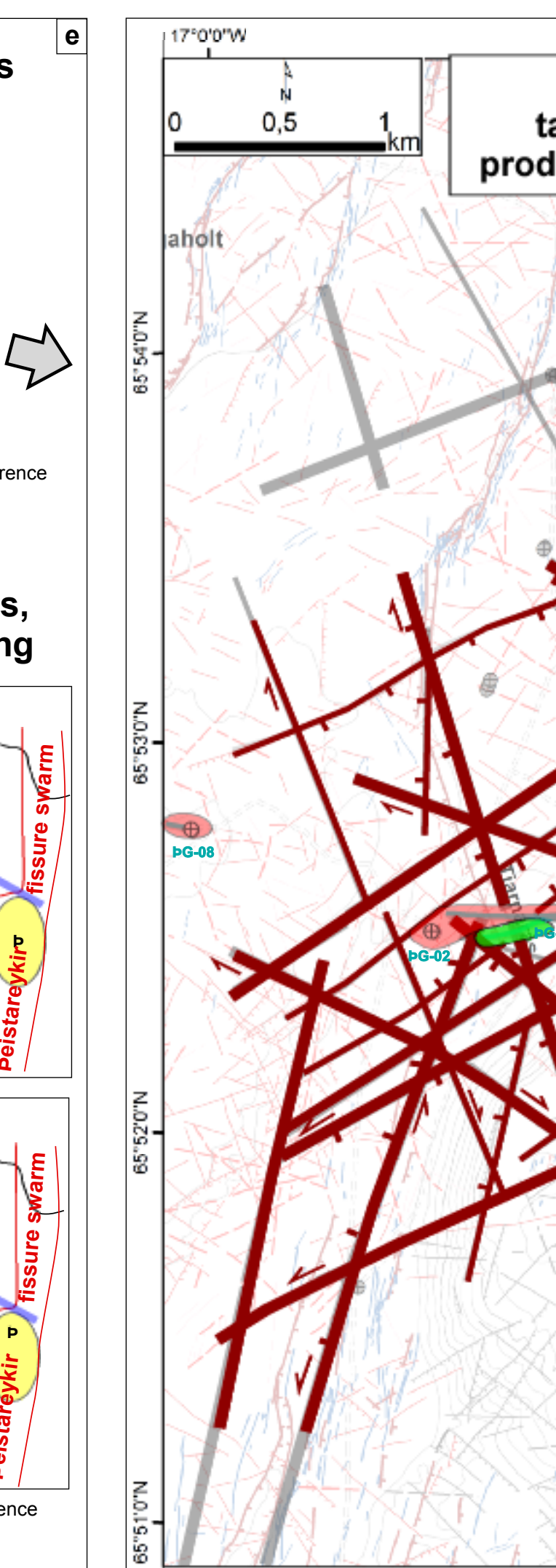


Stress at the plate boundaries

Modified from Garcia et al., (2002). See text for full reference

Local stress fields variations, normal and strike-slip faulting

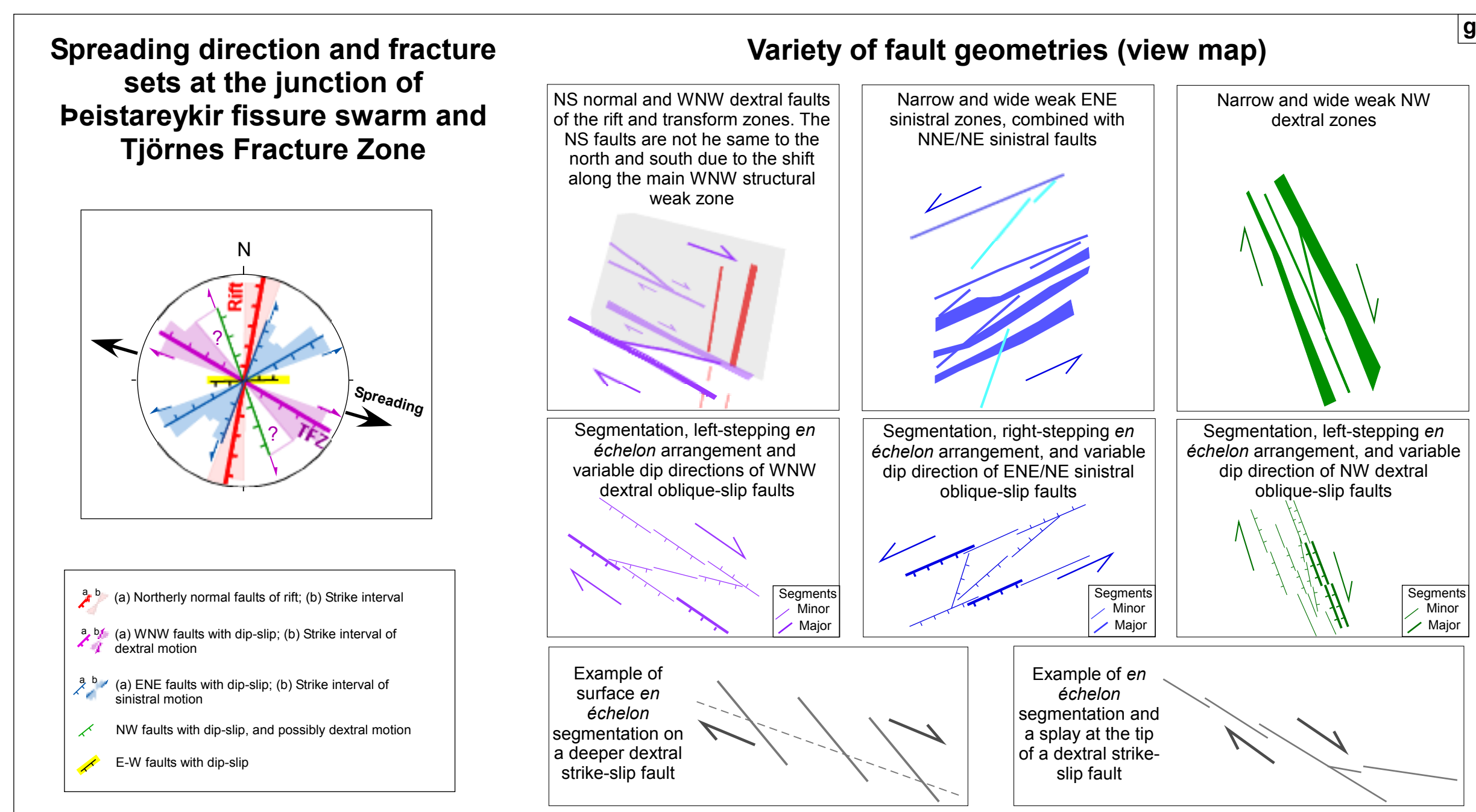
Modified from Homberg et al., (2010). See text for full reference



Spreading direction and fracture sets at the junction of Peistareykir fissure swarm and Tjörnes Fracture Zone

Variety of fault geometries (view map)

- NS normal and WNW dextral faults of the rift and transform zones. The NS faults are not the same to the north and south due to the shift along the main WNW structural weak zone
- Narrow and wide weak ENE sinistral zones, combined with NNE/ENE sinistral faults
- Narrow and wide weak NW dextral zones
- Segmentation, left-stepping en échelon arrangement and variable dip directions of WNW dextral oblique-slip faults
- Segmentation, right-stepping en échelon arrangement, and variable dip direction of ENE/ENE sinistral oblique-slip faults
- Segmentation, left-stepping en échelon arrangement, and variable dip direction of NW dextral oblique-slip faults
- Example of surface en échelon segmentation on a deeper dextral strike-slip fault
- Example of en échelon segmentation and a splay at the tip of a dextral strike-slip fault



Multidisciplinary structural model of Peistareykir geothermal field, potential drilling targets, and fault geometry

Refer to this map as:
Maryam Khodayar
Sveinbjörn Björnsson
Sigurður Garðar Kristinnsson
Ragna Karlsdóttir
Magnús Ólafsson

Report ISOR-2015/043



Landsvirkjun

Háaleitisbraut 68
103 Reykjavík
landsvirkjun.is

landsvirkjun@lv.is
Sími: 515 90 00

